

The Flat Spectrum Radio Luminosity Function, Gravitational Lensing, Galaxy Ellipticities and Cosmology

C.S. Kochanek

Harvard-Smithsonian Center for Astrophysics, MS-51
60 Garden Street
Cambridge MA 02138

ABSTRACT

The number of lenses found in the JVAS survey of flat-spectrum radio sources for gravitational lenses is consistent with statistical models of optical surveys for lensed quasars. The 90% confidence limit on Ω_0 in flat cosmological models ($\Omega_0 + \lambda_0 = 1$) is approximately $0.15 \lesssim \Omega_0 \lesssim 2$. Depending on the RLF model, we predict 2.4 to 3.6 lenses in the JVAS survey and in the first part of the fainter CLASS survey, and 0.3 to 0.6 lenses in the brighter PHFS survey for an $\Omega_0 = 1$ model. The uncertainties are due to the small numbers of lenses (there are only 4 compact JVAS lenses) and the uncertainties in the radio luminosity function (RLF) caused by the lack of information on the redshift distribution of 10-300 mJy radio sources. If we force the models to produce the observed number of JVAS lenses, the mean redshift of a 50 mJy source varies from $z_s = 0.4$ for $\Omega_0 = 0$, to 1.9 for $\Omega_0 = 1$, to almost 4.0 for $\Omega_0 = 2$ when $\Omega_0 + \lambda_0 = 1$. The source fluxes and redshifts of the lenses in the JVAS and CLASS surveys are consistent with the statistical models. The numbers of four-image lenses found in the JVAS survey and in surveys for lensed quasars are mutually consistent, but slightly larger than expected for models using the observed axis ratios of E and S0 galaxies. The best fits to the lens data require a projected axis ratio of $b/a = 0.50$ with a 90% confidence range of $0.25 < b/a < 0.65$.

Subject headings: cosmology: theory – dark matter – gravitational lensing – galaxies: structure – galaxies: elliptical and lenticular – radio sources – radio source counts

1. Introduction

The number of gravitational lenses found in systematic surveys for lenses is a strong constraint on cosmological models, particularly models with a large cosmological constant (Turner 1990, Fukugita, Futamase & Kasai 1990). Quantitative analyses of surveys for multiply imaged quasars (Kochanek 1993, 1996, Maoz & Rix 1993) currently give a formal two standard deviation (2σ) upper limit on the cosmological constant of $\lambda_0 < 0.66$, effectively ruling out values large enough to be cosmologically interesting. The published optical samples contain 862 quasars and 5 lenses produced by galaxies. The λ_0 limit includes all the statistical uncertainties in the model (the number of lenses, galaxy luminosity function, dynamical normalizations and the quasar number counts), and is insensitive to the mass distribution of the lens galaxies. Galaxy evolution weakly affects the limit (Mao 1991, Mao & Kochanek 1994, Rix et al. 1994) because physical models of galaxy mergers generally preserve the expected number of lenses. Moreover, gravitational lensing depends on the properties of low redshift elliptical galaxies ($z < 1$) even if $\lambda_0 = 1$, and recent observations show little evolution in this population (e.g. Lilly et al. 1995, Dickinson 1995, Driver et al. 1995). For bright quasars the selection effects of the survey to find the quasars are probably unimportant (Kochanek 1991, 1996), although this issue should be reexamined. Kochanek (1993) found no detectable bias in the lens sample between radio, color, and spectrally selected quasars. Absorption by dust in the lens galaxies can strongly affect the statistical models (Kochanek 1991, 1996, Tomita 1995), but the current dust content of E/S0 galaxies is far too low to alter the statistics. Nonetheless, absorption can be a large systematic problem in the optically selected lens samples, and there is evidence in some of the radio lenses (e.g. Lawrence et al. 1994) for high extinction.

Most of the known lenses produced by galaxies were not found by surveying quasars at optical wavelengths, but by surveying radio sources. The largest number have been found in the MIT/Greenbank or MG survey (Burke et al. 1992), which has found six lenses. The MG survey examines all radio sources exceeding a flux limit of 50 mJy (see Lehár 1991), and the resulting lens sample is dominated by extended steep spectrum sources that form radio ring lenses such as MG1131+045 (Hewitt et al. 1988). The extended structure of steep spectrum sources complicates statistical analyses because the finite size of the sources strongly modifies the lensing probability (Kochanek & Lawrence 1990). The Jodrell Bank-VLA Astrometric Survey (JVAS, Patnaik 1994, Patnaik et al. 1992, King et al. 1996, King & Browne 1996), CLASS (Jackson et al. 1995, Myers et al. 1995, Myers 1996), and PHFS (Webster et al. 1996) surveys are restricted to flat spectrum radio sources. Flat spectrum sources are generally compact radio cores, making it much simpler to recognize lensed systems and to compute their statistics. The JVAS sample consists of 2200 sources brighter than 200 mJy. It contains five lenses, two doubles (B 0218+357 and a

candidate), two quads (MG 0414+0534 and B 1422+231), and one hybrid (B 1938+666). The published subset of the CLASS survey has 676 sources brighter than 25 mJy and 2575 sources brighter than 50 mJy. It contains at least one double (CLASS 1600+434) and one quad (CLASS 1608+656). The PHFS survey has 323 sources brighter than 500 mJy, and no lensing results are known.

There are many advantages to studying the statistics of radio lens surveys rather than optical quasar lens surveys. The radio samples are selected purely on their radio flux and spectral index, so there is almost no imaginable bias against including lenses in the sample. The radio samples are immune to the effects of dust extinction in lens galaxies. The radio surveys are very uniform and typically have better resolution than quasar surveys. In short, the radio surveys avoid many of the systematic errors that may bias the conclusions of the statistical models for lensed quasars. The redshift and flux distributions of the radio samples are different from that of the quasar samples, so statistical consistency between the radio and quasar lens samples is a good check of the reliability of statistical models. The only systematic errors common to both the radio and quasar surveys are the number and mass distributions of lens galaxies. Both of these systematic errors are best addressed by finding larger numbers of lenses.

The radio sources are not a panacea of course. The problem for the radio surveys is the relative paucity (compared to quasar samples) of information on the luminosity function of radio sources as a function of redshift. While the number counts of radio sources are well determined (see reviews by Dunlop 1994, Windhorst, Mathis & Neuschaeffer 1990, Kellerman & Wall 1987), complete redshift surveys exist only for bright radio sources ($S_5 \gtrsim 1$ Jy), although there are moderately complete surveys for somewhat fainter sources ($S_5 \gtrsim 0.1$ Jy). Since most of the radio lens surveys use flux limits of 25-500 mJy, the source of a typical lens comes from the flux ranges where there is little redshift information. Thus the dominant uncertainty in statistical models of radio lenses is the redshift distribution or luminosity function of the sources. An important goal of this study is to determine the observations that can eliminate this source of uncertainty in the lens calculations.

King et al. (1996) and King & Browne (1996) pointed out that the numbers of four-image lens systems in the JVAS sample is anomalously high. Where their models, based on the Dunlop & Peacock (1990) RLF, predicted that 1 in 6 lenses would be a four-image lens, the JVAS sample actually contains 2 two-image lenses, 2 four-image lenses, and one hybrid. An examination of elliptical models for quasar surveys (Kochanek 1991, Wallington & Narayan 1993, Kasiola & Kovner 1993) also suggests the need for very elliptical models to make four-image systems dominate the sample of bright quasar lenses, and models of individual lenses (e.g. Kochanek 1991, Ratnatunga et al. 1995) can also be

very elliptical. These are all aspects of what Schechter (1996) refers to as the “ellipticity crisis” in gravitational lensing. The only plausible solutions suggested to the problem have been that it is a statistical fluke, that is caused by systematic errors in lens and selection effects models, or that the extra shear is induced by potential fluctuations along the path from the observer to the source. Calculations by Bar-Kana (1996) show that the extra shear generated by large scale structure may be large enough to produce the observed effects, although more detailed calculations are needed.

Most of this study is devoted to methods for determining the radio luminosity function (RLF) of flat spectrum radio sources so that we can probe the effects of its uncertainties on the statistics of gravitational lenses. In §2 we summarize the data on radio number counts and redshift surveys, and describe the statistical methods used to fit the RLF to the data. In §3 we discuss the lensing calculation and develop models for the statistics of elliptical (density) singular isothermal spheres. In §4 we explore the RLF, lens statistics, and cosmology for flat models with a cosmological constant, considering only the total numbers of lenses and not their relative morphologies. In §5 we explore the effects of forcing the models to produce exactly the number of lenses observed in the JVAS survey. In §6 we consider the relative numbers of two- and four-image lenses expected in the surveys and quantify the extent of the “ellipticity crisis”. In §7 we summarize our conclusions and discuss the data required to reduce the uncertainties.

2. The Radio Luminosity Function

In this section we summarize the constraints on the RLF of flat spectrum sources and develop a computational method for determining the RLF using linear regularization. If $S_\nu \propto \nu^{-\alpha}$, then flat spectrum is defined by $\alpha < 0.5$, and the spectral index α for the sources in the lens surveys was usually measured between 2.7 GHz and 5 GHz. The RLF is a two-dimensional function of redshift and flux or luminosity, and fully determining the RLF requires the redshift distribution of sources at all fluxes of interest. In practice, we know the number counts, the integral of the RLF over source redshift at fixed flux, over a very wide range of fluxes from $10 \mu\text{Jy}$ to 10^2 Jy with reasonable accuracy, and the redshift distributions of bright sources ($S_5 > 0.3 \text{ Jy}$). There are weak, and systematically suspect, constraints on the local RLF of fainter radio sources. Because of the limitations from these data, the redshift distribution of sources fainter than 0.3 Jy is largely determined by assumptions about the structure of the RLF such as smoothness and evolution. In this section we develop a method that will allow us to explore the effects of these uncertainties on the expected number of lenses in the flat spectrum samples. There are, of course, many

studies of the RLF made with the goal of understanding the evolution of radio sources in luminosity and density (e.g. Condon 1989, Peacock 1985, Kellerman & Wall 1987, Windhorst et al. 1990, Dunlop & Peacock 1990, Dunlop 1994). Generally, these RLF models are not well designed for studies of gravitational lenses because of their assumptions about unmeasured redshifts in redshift surveys of radio sources. We use the Dunlop & Peacock (1990) pure-luminosity evolution model as our point of comparison to these earlier works.

2.1. Sources of Data

We build the RLF from three elements: number counts as a function of flux, estimates of the local RLF, and limited redshift surveys. We collated the 5 GHz number counts from Altschuler (1986), Bennett et al. (1985), Donnelly et al. (1987), Fomalont et al. (1984), Fomalont et al. (1991), Gregory & Condon (1981), Maslowski et al. (1981), Pauliny-Toth et al. (1978), and Wrobel & Krause (1990) and the 5 GHz flat spectrum number counts from Condon & Ledden (1981), Donnelly et al. (1987), Fomalont et al. (1984), Fomalont et al. (1991), Owen et al. (1983), Pauliny-Toth et al. (1978) and Witzel et al. (1979). The data for the flat spectrum counts are more limited than the overall number counts, so we fit the fraction of the sources that have a flat spectrum as a function of flux S with a low order polynomial in $\log S$ and then correct the overall counts using the estimated fraction. The errors in the differential number counts were broadened to include the statistical and fit errors for the fraction of flat spectrum sources. We use this method because the fraction of flat spectrum sources is only measured in averages over large flux ranges, but varies slowly with flux (it ranges from ~ 0.25 to ~ 0.5). We avoid over-smoothing the counts by fitting the fraction of sources that are flat and then correcting the total counts.

The local RLF is determined from a combination of the complete redshift surveys of bright radio sources and radio surveys of optical magnitude limited samples of nearby galaxies. The latter surveys constrain the local RLF in the observed flux range from ~ 10 mJy to ~ 500 mJy. We use the models of Toffolatti et al. (1987) and Dunlop & Peacock (1990). The faint local RLF data have large statistical and systematic errors as there are few nearby flat-spectrum sources, and the data are derived from heterogeneous optical magnitude and galaxy-type limited surveys. We tried models without the local RLF constraints, and these models show significantly larger variations in the expected number of lenses.

There are nearly complete redshift surveys of flat spectrum radio sources for fluxes $S_{2.7} > 1.5$ Jy from Peacock & Wall (1981) and Wall & Peacock (1985). We assumed a

spectral index of $\alpha = 0$ for the compact sources ($S_\nu \propto \nu^{-\alpha}$) to convert the 2.7 GHz fluxes to 5 GHz following Dunlop & Peacock (1990). We divided the data into three samples for the flux ranges from $3 \text{ Jy} < S_{2.7} < 10 \text{ Jy}$ (34 sources, 33 redshifts), $2 \text{ Jy} < S_{2.7} < 3 \text{ Jy}$ (37 sources, 36 redshifts), and $1.5 \text{ Jy} < S_{2.7} < 2 \text{ Jy}$ (31 sources, 29 redshifts). The missing redshifts in these bright source surveys are usually BL Lac objects with featureless spectra. The number of sources appears small because we include only the flat-spectrum subsets of larger surveys. For fainter sources the redshift surveys are very incomplete. From Peacock (1985) we have a sample with $0.5 \text{ Jy} < S_{2.7} < 1.5 \text{ Jy}$ (40 sources, 30 redshifts), and from the Parkes Selected Area Survey (PSAS, Dunlop et al. 1986, Dunlop et al. 1989, Allington-Smith, Peacock & Dunlop 1991) we have a sample with $0.1 \text{ Jy} < S_{2.7} < 0.5 \text{ Jy}$ (34 sources, 21 redshifts). The CJI survey (Polatidis et al. (1995), Thakkar et al. (1995), Xu et al. (1995)) has the flux range $0.7 \text{ Jy} < S_5 < 1.3 \text{ Jy}$ (73 sources, 59 redshifts), and the CJII survey (Taylor et al. 1994, Henstock et al. 1995, Henstock, Browne, & Wilkinson 1994) has the flux range $0.35 \text{ Jy} < S_5 < 0.7 \text{ Jy}$ (187 sources, 137 redshifts). The Parkes Half-Jansky Flat-Spectrum Sample (PHFS, Webster et al. 1995) with $S_{2.7} > 0.5 \text{ Jy}$ (323 sources, 258 redshifts) is available only as a redshift histogram for the entire sample. We did not use the PHFS sample because of its incompleteness, lack of flux information, and because it probably has a large overlap with the other high flux samples. For each survey where we could identify the objects, we used NED¹ to fill in any redshifts found after the original publication.

In both the number counts data and the redshift data there is some double counting of sources, so the samples from different studies are not fully statistically independent. Such double counting gives extra weight to some measurements, but should not significantly bias our final results. Moreover, we cannot eliminate double counting in the redshift distributions for the binned samples (like CJII) because we were unable to obtain the source and redshift lists.

2.2. Numerical Method

Rather than fitting a parametric form for the luminosity function, we will simply determine the two-dimensional luminosity function in redshift and flux $\rho = dN/dV d \ln S$ where dV is the comoving volume element, and S is the observed 5 GHz flux (in Jy). The luminosity of the source (W Hz^{-1}) at the 5 GHz *rest* frequency is $L = 4\pi S D_{OS}^2 (1+z)^{1+\alpha}$ if

¹The NASA/IPAC Extragalactic Database (NED) is a project of the Jet Propulsion Laboratory, at the California Institute of Technology, under contract with NASA.

the spectrum is $S_\nu \propto \nu^{-\alpha}$ and $(1+z)D_{OS}$ is the luminosity distance to the source. We use flux rather than luminosity to describe the RLF to minimize the effects of cosmology and variations in the spectral index.

The RLF is specified on a grid in redshift and flux, where $\rho_{ij} = dN/dV d \ln S(z_i, S_j)$ is the mean comoving source density in the redshift range $z_{i-1/2} < z < z_{i+1/2}$ and in the flux range $S_{j-1/2} < S < S_{j+1/2}$. The flux zones are uniform in $\ln S$ with $j = 1 \cdots N_S$ and $S_{1/2} = 10 \mu\text{Jy}$ and $S_{N_S+1/2} = 10 \text{ Jy}$ with $N_S = 101$. The j^{th} zone is centered at flux $S_j = (S_{j+1/2}S_{j-1/2})^{1/2}$. Some physical constraints we try to impose on the RLF model, such as a constant comoving density of sources, must compare source densities at fixed luminosity density rather than fixed flux. We made a special choice for the redshift grid to simplify such calculations. The luminosity of a source with flux S_j at redshift z_i is $L_{ij} = 4\pi S_j D_{OS}^2(z_i)(1+z_i)^{1+\alpha}$. We define the redshift zones by the requirement that $L_{ij} = L_{i-1j+1}$, so that a line of constant luminosity crosses the redshift-flux grid at 45° to the lines of constant flux. This requirement leads to redshift zones that are roughly logarithmic in z_i , with $z_1 = 0.01$, $z_{N_z} = 5.16$, and $N_z = 110$ zones for $N_S = 101$. The source density is assumed to be zero for higher redshifts, but we did not force any regularity constraint at the redshift cutoff. The comoving volume element is $dV = 4\pi D_{OS}^2 dD_{OS}$ for flat cosmologies (see Carroll, Press, & Turner 1992, eqn. (12)). Let the comoving volume between redshift zero and $z_{i+1/2}$ be $V_{i+1/2}$, so that the comoving volume element between redshifts $z_{i-1/2}$ and $z_{i+1/2}$ is $\Delta V_i = V_{i+1/2} - V_{i-1/2}$. The logarithmic flux volume element at flux S_j is $\Delta \mathcal{F}_j = \ln S_{j+1/2}/S_{j-1/2}$. We use the numerical variable α_{ij} with $\rho_{ij} = \exp(\alpha_{ij})$ to force the RLF to be positive definite.

The numerical solution must optimize the fit to the number counts as a function of flux, the local RLF, the redshift surveys of brighter sources, the smoothness of the solution, and the number of lenses. For each term related to the data we calculate an estimate of the likelihood that the model fits the data, and a good model maximizes the likelihood of fitting the data. However, our model has many more degrees of freedom than there are constraints, so we can find models that fit the data nearly perfectly. Such models also have odd wiggles and oscillations because they overfit the statistical fluctuations in the data to achieve perfect agreement. To balance this tendency we add smoothing functions that are designed to be small when the solution is physically reasonable. The smoothing terms drive the solution to show small pixel-to-pixel variations, have larger numbers of faint than bright sources, and show varying amounts of evolution. The procedure we use is linear regularization (see Press et al. 1992). We define L_{data} to behave like a χ^2 statistic, where a perfect fit has $L_{data} = 0$ and a typical good solution has $L_{data} = N_{data}$ where N_{data} is the number of constraints. Viewed as a maximum likelihood problem, we have defined L_{data} to be $L_{data} = -2 \ln(\text{likelihood})$. If U is a concave smoothing function with minimum value

$U = 0$ for a perfectly smooth solution, then our procedure adjusts the RLF to minimize the function

$$F = L_{data} + \lambda_U U \quad (1)$$

for a fixed value of the Lagrangian multiplier λ_U using the conjugate gradient method (see Press et al. 1992). If $\lambda_U = 0$ we optimize only the fit to the data, and we find a solution with $L_{data} \ll N_{data}$ that is not very smooth. In the opposite limit, $\lambda_U \gg 1$, we optimize only the smoothness of the solution to find $U \sim 0$ but $L_{data} \gg N_{data}$. By varying λ_U , we find the smoothest solution that is a statistically reasonable fit to the data with $L_{data} = N_{data} \pm (2N_{data})^{1/2}$. We search the space of reasonable RLFs consistent with the constraints by varying the structure of the smoothing function. Physical results should not (and do not) depend on the exact converged value of L_{data} . In this section we describe the terms for fitting the number counts, the local RLF, the redshift surveys, and the smoothing. In the next section we describe the terms for the lensing data.

The number counts data consists of $k = 1 \cdots N_N = 61$ measurements of the average differential number counts D_k , where

$$D_k = \left\langle \frac{dN}{dS} \right\rangle = \frac{1}{S_{Hk} - S_{Lk}} \int_0^\infty dz \frac{dV}{dz} \int_{S_{Lk}}^{S_{Hk}} \frac{dS}{S} \rho(z, S), \quad (2)$$

and $S_{Lk} < S < S_{Hk}$ is the flux range of the measurement. The measurement uncertainty is e_k . The current numerical model predicts that the average differential flux counts are

$$D_k^M = \frac{1}{S_{Hk} - S_{Lk}} \sum_{i=1}^{N_z} \sum_{j=j_{min}}^{j_{max}} \rho_{ij} \Delta V_i \ln \left[\frac{\min(S_{Hk}, S_{j+1/2})}{\max(S_{Lk}, S_{j-1/2})} \right] \quad (3)$$

where the limits of the flux summation are the flux zones bracketing the constraint ($S_{j_{min}-1/2} < S_{Lk} < S_{j_{min}+1/2}$ and $S_{j_{max}-1/2} < S_{Hk} < S_{j_{max}+1/2}$), and the limits of the redshift summation cover all redshifts. The numerical integral in eqn. (3) uses a 0th-order approximation, because it does no interpolation of the density values. Numerical experiments showed that the grid resolution was high enough to avoid using more complicated, higher order integration methods. We estimate the likelihood of the model fitting the number counts data with a χ^2 statistic,

$$\chi_N^2 = \sum_{k=1}^{N_N} \left(\frac{D_k - D_k^M}{e_k} \right)^2, \quad (4)$$

where we expect a good solution to have $\chi_N^2 = N_N \pm (2N_N)^{1/2}$. The constraints extend from 10 μ Jy to 10 Jy, and we have no need to extrapolate to higher or lower fluxes than are constrained by the number counts data. The local RLF simply specifies the mean value of

ρ_{ij} over some flux range to some low redshift limit (e.g. 0.07 for Toffolatti et al. 1987). This leads to a χ_L^2 for fitting the local RLF in which the redshift summations of eqn. (3) extend only to the redshift limit of the local RLF. Although we use 10 data in the local RLF constraints, forcing $\chi_L^2 = 10$ represents an overfitting of the local RLF data. The RLF data should not be modeled using a χ^2 distribution because the data for each point are derived from small numbers of sources (0 to 5). Broader Poisson uncertainties would be more appropriate, but we were forced to use a χ^2 statistic by the format of the published local RLF models. We also used both the Dunlop & Peacock (1990) and Toffolatti et al. (1987) models simultaneously to include the uncertainties from their differing interpretations of the same data.

We fit the redshift surveys using binned data. Binning the data is cruder than the two-dimensional Kolmogorov-Smirnov test developed and used by Peacock (1983) and Dunlop & Peacock (1990), but adequate for our purposes. Moreover, some of the redshift constraints are available only in binned forms (the PHFS and CJII samples). We divided the various samples used by Wall & Peacock (1985) and Dunlop & Peacock (1990) into flux ranges and added the CJI and CJII samples to give a total of $k = 1 \cdots 7$ redshift surveys whose properties are summarized in §2.1. Survey k has N_{Zk} measured redshifts and N_{Ok} objects between fluxes $S_{Lk} < S < S_{Hk}$. The number of measured redshifts is generally less than the number of objects, so the mean completeness of a survey is N_{Zk}/N_{Ok} . Survey k is divided into $l = 1 \cdots N_k$ redshift bins bounded by $z_{Lkl} < z < z_{Hkl}$ (and $z_{Lkl} = z_{Hkl-1}$), and bin l of survey k contains N_{kl} objects with measured redshifts ($\sum_{l=1}^{N_k} N_{kl} = N_{Zk}$). To compare the model to the redshift data we must normalize the model to match the number of objects of the survey, and correct for incompleteness.

Let A_k be the “effective area” of survey k , and let f_{kij} be the probability that a redshift is measurable for a source at redshift z_i with flux S_j in survey k . For simplicity we assumed that the redshift completeness in a given survey does not depend on the radio flux, so that $f_{kij} = f_{ki}$. The “effective area” is determined by the constraint that the total number of objects N_{Ok} must match the flux counts,

$$N_{Ok} = A_k \int_0^\infty dz \frac{dV}{dz} \int_{S_{Lk}}^{S_{Hk}} \frac{dS}{S} \rho = A_k \sum_{i=1}^{N_z} \sum_{j=j_{min}}^{j_{max}} \rho_{ij} \Delta V_i \ln \left[\frac{\min(S_{Hk}, S_{j+1/2})}{\max(S_{Lk}, S_{j-1/2})} \right]. \quad (5)$$

The number of objects with measured redshifts in bin l is

$$N_{kl}^M = A_k \sum_{i=i_{min}}^{i_{max}} \sum_{j=j_{min}}^{j_{max}} f_{ki} \rho_{ij} \left[\min(V_{Hkl}, V_{i+1/2}) - \max(V_{Lkl}, V_{i-1/2}) \right] \ln \left[\frac{\min(S_{Hk}, S_{j+1/2})}{\max(S_{Lk}, S_{j-1/2})} \right] \quad (6)$$

subject to the constraint that $N_{Zk} = \sum_{l=1}^{N_k} N_{kl}^M$. V_{Lkl} and V_{Hkl} are the comoving volumes for

redshifts less than z_{Lkl} and z_{Hkl} respectively, and i_{min} and i_{max} are defined to be the zones bracketing redshift bin l (i.e., $z_{i_{min}-1/2} < z_{Lkl} < z_{i_{min}+1/2}$).

Dunlop & Peacock (1990) relied on redshift-magnitude relations, or simply assumed an intermediate redshift for the objects without measured redshifts. This is not adequate for a lensing calculation because the lensing probabilities vary strongly with redshift for $z > 1$ where the scatter in the redshift-magnitude relations is too large to make them useful predictors. We instead parametrize our uncertainties through a completeness model defined by the f_{ki} , and plead for better redshift surveys in the conclusions.

We treated two simple cases. In the *uniform completeness* model (labeled by $C = 0$ in Table 1), we assume that the completeness is independent of redshift, $f_{ki} = f_k$, and that the measured redshifts are an unbiased representation of the redshift distribution. The probability of measuring any redshift is simply the average completeness of the sample, $f_k = N_{Zk}/N_{Ok}$. In the *linear completeness model* (labeled by $C = 1$ in Table 1), $f_{ki} = a + bz_i$ with $b < 0$ so that the completeness declines with redshift. If $\langle z_k \rangle$ is the mean redshift predicted by the model, then we use $a = 1$ and $b = -(N_{Ok} - N_{Zk})/(N_{Ok}\langle z_k \rangle)$. The model for f_{ki} must be modified if the detectable fraction becomes negative at the maximum redshift, $f_{kN_z} < 0$ at $z_{max} = z_{N_z+1/2}$. When it becomes negative, we must drop the assumption that the completeness is unity at zero redshift ($a = 1$), and instead use the coefficients $a = (N_{Zk}/N_{Ok})z_{max}/(z_{max} - \langle z \rangle)$ and $b = -a/z_{max}$. The two completeness models have negligible differences in nearly complete surveys, but the linear completeness model will predict larger numbers of high redshift sources in incomplete surveys.

For a given completeness model, we compare the predicted number of measured redshifts N_{kl}^M to the measured number N_{kl} . We do this using the logarithm of the Poisson maximum likelihood ratio for that point,

$$L_{kl} = N_{kl} \ln \frac{N_{kl}^M}{N_{kl}} - N_{kl}^M + N_{kl} \quad (7)$$

so that when $N_{kl}^M = N_{kl}$, $L_{kl} = 0$. If we take the weighted average of L_{kl} over the Poisson likelihood function, we find that the mean value of the likelihood is $\langle L_{kl} \rangle = -0.5$ for $N_{kl} \gg 1$. For $N_{kl} = 0, 1$, and 2 , we find $\langle L_{kl} \rangle = -1, -0.58$, and -0.54 respectively. The total likelihood of fitting redshift survey k is

$$L_k = \sum_{l=1}^{N_k} L_{kl}. \quad (8)$$

The function L_{data} is equal to $-2\ln(\text{likelihood})$, so to give equal statistical weight to the redshift data and the number counts we add $-2L_k$ to L_{data} .

The final terms of the function F (eqn. (1)) are designed to produce a smooth model. We must add such terms because the number counts, redshift, and lens constraints are not sufficient to determine fully the density of sources at all redshifts and fluxes – the data are noisy, and redshift surveys are available only for bright sources ($S \gtrsim 300$ mJy). By construction the solution is positive definite and/or monotonic depending on whether we use α_{ij} or β_{ij} as the numerical variable. We introduce terms to bias the solution to a smoothly increasing number of sources at fainter fluxes and either no evolution or strong evolution at fixed luminosity. The first smoothing term biases the solution to a slope of $\rho \propto S^{-\xi}$ at a fixed redshift, by adding the function

$$U_1 = \sum_{i=1}^{N_z} \sum_{j=1}^{N_f-1} [\alpha_{ij} - \alpha_{ij+1} - \xi \ln(S_{j+1}/S_j)]^2 \quad (9)$$

where our standard model uses the “Euclidean slope” of $\xi = 1.5$. The second term biases the solution to a constant comoving luminosity function by adding

$$U_2 = \sum_{i=2}^{N_z} \sum_{j=1}^{N_S-1} \frac{1}{1 + \kappa w_{i-1/2}} [\alpha_{ij} - \alpha_{i-1j+1}]^2. \quad (10)$$

The third term biases the solution to constant comoving density at fixed flux rather than fixed luminosity

$$U_3 = \sum_{i=2}^{N_z} \sum_{j=1}^{N_S} \frac{\kappa w_{i-1/2}}{1 + \kappa w_{i-1/2}} [\alpha_{ij} - \alpha_{i-1j}]^2. \quad (11)$$

where $w_{i-1/2}$ is the ratio of the difference in time between redshifts z_i and z_{i-1} in units of the local Hubble time to the difference in time in units of the local Hubble time for redshift zones N_z and $N_z - 1$, and κ is a constant. We must introduce some weighting factor $w_{i+1/2}$ because the redshift zones are (approximately) logarithmically spaced, and uniform weighting allows too much evolution at low redshift. At redshift z , $w(z)^{-1} \simeq 1 + 1/3((1+z)^{1/2} - 1)$, and $\kappa w(z) = 1$ at $z_c \simeq (6\kappa - 5)/9(\kappa - 1)^2$. The term U_2 controls the smoothing for $z \lesssim z_c$, and the term U_3 controls the smoothing for $z \gtrsim z_c$. The larger κ becomes, the stronger the bias towards luminosity evolution at lower redshifts. These terms do not represent all possible, physical smoothing terms, and in §5 we explore treating the lensing terms introduced in §3 as a type of regularizing term.

In summary, the constraint term appearing in the function F is $L_{data} = \chi_N^2 + \chi_L^2 - 2 \sum_{k=1}^7 L_k$ and the smoothing term is $U = U_1 + U_2 + U_3$. There are a total of 147 constraints, so we find the smoothest solutions with $L_{data} = 147$ for different combinations of the constants in the smoothing terms (ξ and κ) and for the two different completeness models. We made one simplification to reduce the amount of calculation. *The smoothing terms and all the constraints on the RLF except the lensing constraints*

are calculated in a fixed $\Omega_0 = 1$ Einstein-DeSitter cosmology. For the data constraints this has no effect because they only depend on the number per unit redshift and flux ($dN/dz dS = \rho dV/dz$, which is cosmology independent), but the physical meaning of the smoothing constraints varies with cosmology because U_2 and U_3 depend on the luminosity density of the sources.

3. The Lens Model

We use a (density) ellipsoidal singular isothermal sphere for our lens model, characterized by a circular critical radius $b = 4\pi(\sigma/c)^2 D_{LS}/D_{OS}$ and an ellipsoidal parameter ϵ (see Kassiola & Kovner 1993). The surface density axis ratio of the model is $b/a = (1 - \epsilon)^{1/2}/(1 + \epsilon)^{1/2}$. The circular critical radius b depends on the (dark-matter) velocity dispersion σ and the ratio of the distances from the lens to the source and from the observer to the source. In a flat cosmology ($\Omega_0 + \lambda_0 = 1$), the distances are defined by

$$D_{12} = \frac{c}{H_0} \int_{z_1}^{z_2} dz \left[(1+z)^2 (1 + \Omega_0 z) - z(2+z)\lambda_0 \right]^{-1/2} \quad (12)$$

(Carroll, Press, & Turner 1992) where Ω_0 and λ_0 are the matter density and the cosmological constant. If the lower redshift $z_1 = 0$, these are proper motion distances. The lens equations are

$$u = x - \frac{b}{\sqrt{2\epsilon}} \tan^{-1} \left[\frac{\sqrt{2\epsilon} \cos \theta}{(1 - \epsilon \cos 2\theta)^{1/2}} \right] \quad (13)$$

$$v = y - \frac{b}{\sqrt{2\epsilon}} \tanh^{-1} \left[\frac{\sqrt{2\epsilon} \sin \theta}{(1 - \epsilon \cos 2\theta)^{1/2}} \right] \quad (14)$$

where u, v are the source coordinates, x, y are Cartesian image coordinates, and r, θ are polar image coordinates. The magnification has a remarkably simple form,

$$M^{-1} = 1 - \frac{b}{r} \frac{1}{(1 - \epsilon \cos 2\theta)^{1/2}}, \quad (15)$$

and contours of constant magnification are contours of constant surface mass density. In particular, the axis ratio of the tangential critical line ($M^{-1} = 0$) is the axis ratio of the density.

The lens produces both two- and four-image systems. The cross sections are not expressible in simple analytic forms, although they are easily calculated numerically, and we can express the four-image, two-image and total cross sections as power series in ϵ , with

$$\sigma_4 = \frac{\pi}{6} \epsilon^2 b^2 \left[1 + \frac{21}{20} \epsilon^2 + \frac{57}{56} \epsilon^4 + \frac{187}{192} \epsilon^6 \dots \right] \quad (16)$$

$$\sigma_2 = \sigma_t - \sigma_4 \quad \text{and} \quad (17)$$

$$\sigma_t = \pi b^2 \left[1 + \frac{1}{3}\epsilon^2 + \frac{1}{5}\epsilon^4 + \frac{1}{7}\epsilon^6 \cdots \right]. \quad (18)$$

These expressions are accurate to 5% or better for $b/a \lesssim 0.4$ ($\epsilon \lesssim 0.7$), and they are invalid beyond $\epsilon > 0.73097$ where the astroid caustic first pierces the radial (pseudo) caustic.

From the properties of the tangential critical line (where $M^{-1} = 0$) we can determine the asymptotic cross sections as a function of magnification (see Blandford & Narayan 1986). The asymptotic cross section for four-image systems with magnification greater than M is

$$\sigma_4(> M) = \frac{4\pi b^2}{(1 - \epsilon^2)^{1/2}} \frac{1}{M^2} \quad \text{for } M \gg 1 \quad (19)$$

and the asymptotic cross section for two-image systems with magnification greater than M is

$$\sigma_2(> M) = \frac{16b^2}{5\sqrt{3}\epsilon} \left[(1 + \epsilon)^{-1/2} + (1 - \epsilon)^{-1/2} \right] \frac{1}{M^{5/2}} \quad \text{for } M \gg 1 \quad (20)$$

and these expressions are valid for $\epsilon < 0.73097$.

We calculated the integral cross sections $\sigma_2(> M, r)$ and $\sigma_4(> M, r)$ numerically for total magnifications greater than M with flux ratios between the brightest and faintest images smaller than $r = 30$. Figure 1 shows the cross sections for galaxies with axis ratios of $b/a = 0.7$ and $b/a = 0.65$ in units of the total cross section of the equivalent circular lens, πb^2 . There is, of course, a distribution of galaxy ellipticities (see Ryden (1992) or Schechter (1987) for examples). We are primarily interested in the distribution for E and S0 galaxies because spirals produce only 15%-20% of lenses (see Kochanek 1996). Moreover, while it is dubious that the ellipticity of the light in E and S0 galaxies is the true ellipticity of the total mass distribution, it is certainly incorrect to assume so for spirals (see the review by Sackett 1996). For simplicity, we will use the average cross sections for the axis ratio range $b/a = 1$ to $b/a = 0.5$ as our basic model, and the integral cross sections for this model are also shown in Figure 1. The average four-image cross section is comparable to that of a galaxy with $b/a = 0.65$ even though the average galaxy has only $b/a = 0.75$ because the four-image cross section is $\propto \epsilon^2$. For this treatment we ignore the question of whether the normalization of the potential b depends on the ellipticity, and in §6 we examine the issue of the mean ellipticity required to fit lens data in more detail.

Let $\hat{P}_2(> M, r) = \sigma_2(> M, r)/\pi b^2$ and $\hat{P}_4(> M, r) = \sigma_4(> M, r)/\pi b^2$ be the probability that a two- or four-image system has total magnification greater than M and a brightest to faintest image flux ratio smaller than r normalized by the cross section of the equivalent circular lens. A convenient property of the singular ellipsoidal isothermal lens is that the structure of the optical depth is unchanged from the singular isothermal sphere. We assume

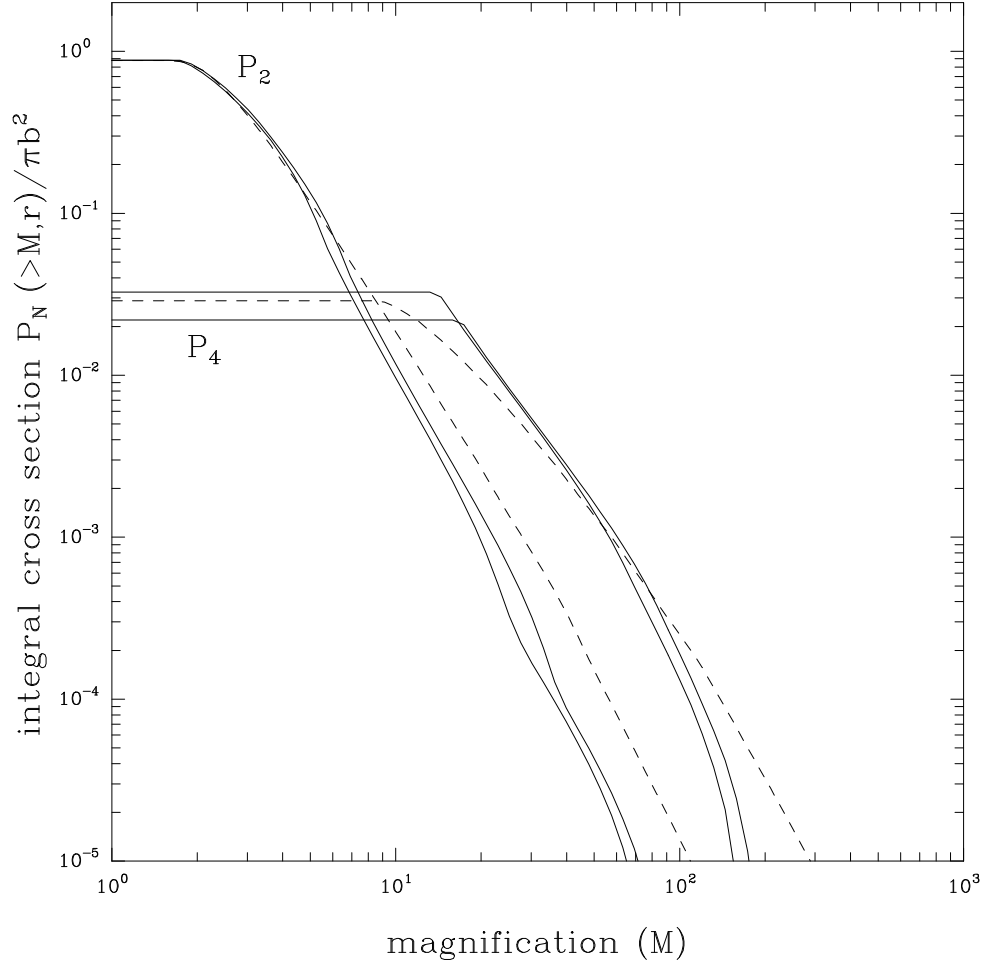


Fig. 1.— Integral cross sections for two- and four-image systems with flux ratios smaller than $r = 30$. The solid lines show the cross sections for $b/a = 0.70$ and $b/a = 0.65$ ellipsoidal isothermal spheres, and the dashed lines show the mean for a uniform distribution of galaxies $0.50 < b/a < 1$, all in units of the cross section for a circular lens πb^2 .

a selection function that detects all images with flux ratios smaller than r in the separation range $\theta_{min} < 2b < \theta_{max}$. We assume a Schechter (1976) function exponent of $\alpha = -1$ and a Faber-Jackson (1976) exponent of $\gamma = 4$ to describe the number counts of galaxies and the relation between luminosity and the velocity dispersion of the isothermal sphere,

$$\frac{dn}{dL} = \frac{n_*}{L_*} \left[\frac{L}{L_*} \right]^\alpha \exp(-L/L_*) \quad \text{and} \quad \frac{L}{L_*} = \left[\frac{\sigma}{\sigma_*} \right]^\gamma, \quad (21)$$

where $n_* = (0.61 \pm 0.21)h^3 10^{-2} \text{ Mpc}^{-3}$ is the local comoving density of E and S0 galaxies (Loveday et al. 1992, Marzke et al. 1994), and $\sigma_* = (220 \pm 20) \text{ km s}^{-1}$ is the (dark-matter) velocity dispersion of an L_* galaxy (Kochanek 1993, 1994, Breimer & Sanders 1993, Franx 1993). The fraction of the lenses that have critical radii in the detectable range is

$$F_a = 30 \int_0^1 dx x^2 (1-x)^2 \left[\exp(-\Delta\theta_{min}^2/\Delta\theta_*^2(1-x)^2) - \exp(-\Delta\theta_{max}^2/\Delta\theta_*^2(1-x)^2) \right] \quad (22)$$

where the characteristic image separation is $\Delta\theta_* = 8\pi(\sigma_*/c)^2 = 2''.8(\sigma_*/220 \text{ km s}^{-1})^2$, and the mean image separation in flat cosmologies is $\Delta\theta_*/2$. The fraction of lenses in the separation range from $\theta_{min} = 0''.3$ to $\theta_{max} = 5''.0$ is $F_a = 0.91$, and the range of separations is large enough to make the value insensitive to large changes in the limits. For $\theta_{min} = 0''.2$, the fraction rises to $F_a = 0.96$, for $\theta_{min} = 0''.4$ it drops to $F_a = 0.87$, for $\theta_{max} = 3''.0$ it drops to $F_a = 0.88$, and for $\theta_{max} = 7''.0$ it rises to $F_a = 0.92$. The optical depth to lensing for circular isothermal spheres in flat cosmologies is $\tau = \tau_*(D_{OS}/r_H)^3/30$ where $r_H = c/H_0$ (Turner 1990). The optical depth scale is $\tau_* = 16\pi^3 n_* r_H^3 (\sigma_*/c)^4 \Gamma[1 + \alpha + 4/\gamma] = 0.024 \pm 0.012$, where the uncertainties are dominated by n_* and σ_* .

We want to determine the number of lenses in a survey of N sources brighter than a flux limit S_0 . As with the redshift surveys, we must first determine the effective area of the survey A_L to normalize the number of sources being examined,

$$N = A_L \int_0^\infty dz \frac{dV}{dz} \int_{S_0}^\infty \frac{dS}{S} \rho(z, S) = A_L \sum_{i=1}^{N_z} \sum_{j=j_{min}}^{N_S} \rho_{ij} \Delta V_i \ln \left[\frac{S_{j+1/2}}{\max(S_0, S_{j-1/2})} \right] \quad (23)$$

where $S_{j_{min}-1/2} < S_0 < S_{j_{min}+1/2}$ brackets the flux limit of the survey. At redshift z_i and flux S_j , the fraction of the sources that are lensed into the survey is just the optical depth $\tau(z_i)$, multiplied by the fraction of lenses with detectable separations F_a , multiplied by the probability that the source is sufficiently magnified to have a flux larger than the survey flux limit $P_n(> S_0/S_j, r)$, where $n = 2$ or 4 for the two-image and four-image lenses respectively. Thus, the expected number of n image lenses is just

$$N_n^M = A_L \sum_{i=1}^{N_z} \sum_{j=1}^{N_S} \rho_{ij} \Delta V_i \Delta \mathcal{F}_j \tau(z_i) F_a P_n(> S_0/S_j, r) \quad (24)$$

including the selection effects on both the separation and the flux ratios. The total number of lenses is $N_T^M = N_2^M + N_4^M$. Remember that in equations (23) and (24), the optical depth $\tau(z_i)$ is computed in the current cosmology, but the two parts of the cosmology independent term $\rho dV/dz$ are computed in an $\Omega_0 = 1$ model. Simple modifications of eqn. (24) can be used to determine the distribution of the lenses in source redshift or flux. Because of the increased complexity and the uncertainties arising from fitting the RLF, we chose not to include the uncertainties in the lens models or the more complicated configuration probabilities used in Kochanek (1993, 1996).

We define the likelihood of fitting the lens data by the logarithm of the Poisson likelihood ratio (as in the redshift survey models of §2.2), with

$$L_L = N_T \ln \frac{N_T^M}{N_T} - N_T^M + N_T \quad (25)$$

rather than using two separate terms for the numbers of two- and four-image lenses. The total number of lenses depends only weakly on the ellipticity, so it is a more robust variable for exploring the cosmological implications of the radio surveys in §4 and §5. We add this likelihood to the overall function with an additional Lagrangian multiplier λ_L that will determine the weight given to the lensing constraint in fitting the RLF,

$$F = \chi_S^2 + \chi_L^2 - 2 \sum_{k=1}^7 L_k + \lambda_U (U_1 + U_2 + U_3) - 2\lambda_L L_L. \quad (26)$$

4. Models Without Lensing Constraints

In this section we consider models constrained to fit only the number counts and redshift data ($\lambda_L = 0$ in eqn. 26). We start from the Dunlop & Peacock (1990) pure luminosity evolution model, and then adjust λ_U until we have a “typical” good fit to the data with $L_{data} = 147$. We have several free parameters to explore in this process: the redshift completeness model, the bias exponent ξ for smoothing term U_1 , the balance κ between U_2 and U_3 , and the background cosmological model. We examine only the total number of lenses in this section, and defer a discussion of the relative numbers of two- and four-image lenses to §6. We do not discuss the form of the RLF *per se*.

Table 1 explores models consistent with the number counts and redshift data under various assumptions about the completeness and the smoothing parameters in an $\Omega_0 = 1$ cosmological model. All the models are converged to fit the data equally well, and no constraint is fit poorly. The initial Dunlop & Peacock (1990) model, labeled 00, is a reasonably good fit to both the number counts and redshift data. It has a value of

Table 1. Results With No Lensing Constraints

Model	Ω_0	C	ξ	κ	JVAS		PHFS		CLASS	
					N_2	N_4	N_2	N_4	N_2	N_4
00	1.0	0	—	—	2.44	0.48	0.36	0.09	2.71	0.44
01	1.0	0	1.5	0	2.22	0.40	0.37	0.09	2.29	0.30
02	1.0	1	1.5	0	2.61	0.45	0.45	0.10	2.60	0.32
03	1.0	1	2.0	0	2.78	0.49	0.47	0.11	2.80	0.34
04	1.0	1	1.0	0	2.82	0.49	0.47	0.11	2.84	0.35
05	1.0	1	1.5	1	3.28	0.61	0.54	0.13	3.46	0.46
06	1.0	1	1.5	2	3.21	0.58	0.54	0.13	3.33	0.44
07	1.0	0	1.5	1	2.76	0.53	0.45	0.11	3.00	0.42
08	1.0	0	1.5	2	2.83	0.54	0.47	0.12	3.06	0.43
09	1.0	0	1.5	3	2.60	0.49	0.44	0.10	2.75	0.38

Note. — $C = 0$ is the uniform redshift completeness model, and $C = 1$ is the linear redshift completeness model. The slope ξ appears in the smoothing term U_1 (eqn. 9), and κ determines the balance between U_2 (eqn. 10) and U_3 (eqn. 11). Larger values of κ drive the solution to greater luminosity evolution. N_2 and N_4 are the expected numbers of two- and four-image systems with flux ratios smaller than $r = 30$, uncorrected for detectable separations (multiply by $F_a = 0.91$) or extended sources (multiply by 0.95).

$L_{data} = 209$, while our target value is $L_{data} = 147$, so the typical constraint is fit within “ 1.5σ ”. The largest discrepancies are in the faint number counts (too few faint sources), and the 0.5 to 1.5 Jy redshift distribution (too few high redshift sources). If the observed redshifts are a fair sample (completeness model 0) or we bias the solution towards no luminosity evolution ($\kappa = 0$), then we find smaller numbers of lenses than in the models with decreasing sample completeness with redshift, or strong luminosity evolution. The slope of the bias function at fixed redshift, ξ , only weakly affects the results. The total number of lenses predicted for the JVAS sample ranges from 2.6 (Model 01) to 3.9 (Model 05), and 14–16% of the total are four-image lenses. For comparison, the Dunlop & Peacock (1990) Model 00 predicts 2.9 lenses, 16% of which are four-image lenses, as also found by King & Browne (1996). The spread in the expected number of lenses in Table 1 is a factor of $3/2$, comparable to the uncertainties from the other components of the lens model (see §3). Presumably the true range is somewhat broader because we explored only a finite number of smoothing terms – we return to this issue in §5.

The numbers in Table 1 were not corrected for the limited range of detectable separations, which we estimated would reduce the number of lenses detected by the factor $F_a = 0.91$ in §3. Our statistical model is for point sources, so we should exclude the 5% of JVAS sources that have extended structure (see Patnaik et al. 1992), and treat the statistics of the 95% of the sources that are unresolved or point-like. The statistics of sources with extended or multiple structure are strongly modified by the effects of the structure (see Kochanek & Lawrence 1990), and the probability of an object in this subpopulation being lensed can be much larger than for a point source of comparable flux. If we drop the extended sources, we must also drop any lenses produced from this population. In the JVAS survey, this means eliminating B 1938+666, a lensed double with at least one extended component. Wherever we quantitatively compare the survey data to the observed numbers of lenses, we include the angular selection factor and eliminate the extended sources. In adopting this simple approach, we assume that the extended sources are otherwise indistinguishable in their redshift and flux distributions from the compact sources. With these corrections, the observed sample contains 4 lenses while we expected to find 2.27 (3.37) lenses in Model 01 (05). The Poisson probabilities are 11% and 18% respectively, compared to a peak Poisson probability of 19.5%. In short, the numbers of lenses found in the JVAS survey are statistically compatible with the best fit lensing model found for the quasar lens surveys and an $\Omega_0 = 1$ cosmological model.

Figure 2 shows the expected number of lenses for Models 01 and 05 in the JVAS, CLASS, and PHFS surveys as a function of the matter density Ω_0 in cosmologies with a cosmological constant, $\Omega_0 + \lambda_0 = 1$. In these models we fixed the redshift and flux distribution of the sources (i.e. $dN/dSdz = (dN/dSdV)(dV/dz)$) not the comoving

luminosity function ($dN/dLdV$). This simplification means that the effective smoothing function changes with the cosmological model, but otherwise does not affect the results. Including the angular selection function and dropping the extended sources, the maximum likelihood cosmological model for the JVAS sample ranges from $\Omega_0 \simeq 0.5$ for Model 01 to $\Omega_0 \simeq 0.85$ for Model 05. The 90% (99%) confidence lower limits are $\Omega_0 \gtrsim 0.2$ ($\gtrsim 0.15$) for Model 01, and $\Omega_0 \gtrsim 0.4$ ($\gtrsim 0.3$) for Model 05. The upper limits are not as well defined. Model 01 has a 90% confidence upper limit of $\Omega_0 \lesssim 1.5$, and Model 05 has a 90% confidence limit of $\Omega_0 \lesssim 2.0$. These limits are consistent with those found from the statistics of lensed (optical) quasars (see Kochanek 1996). Note that the Poisson uncertainties in the cosmological model are comparable to the systematic uncertainties from the structure of the luminosity function. Clearer cosmological limits from the radio surveys will depend on both finding more lenses and more tightly constraining the luminosity function.

Figure 3 shows the expected number of lenses per 10^3 sources brighter than a given flux in several of the models, and the error bars or limits that can be derived for each survey. The number of lenses expected in the CLASS survey is always close to that expected for the JVAS survey. Although the total number of sources in the CLASS survey is larger (3258 versus 2200 sources), they are fainter (a flux limit of 25–50 mJy versus 200 mJy). The weaker magnification bias balances the larger numbers of sources. The PHFS survey is smaller (323 sources) but brighter (0.5 Jy) than the JVAS survey. Although the magnification bias is somewhat larger than in the JVAS survey, the number of sources is so much smaller that we typically expect only 0.3–0.6 lenses in the PHFS survey. The flattening probability of finding four-image lenses near 10 mJy is caused by the steepening of the number counts near 0.1–10 mJy.

We now want to explore methods of distinguishing the various RLF models so that the cosmological uncertainties can be reduced. The direct approach is to complete old or conduct new redshift surveys of radio sources. Figure 4 shows the *unlensed* flux distribution of lensed sources in Model 01 for the three surveys. The distribution shows little variation with model. In each case, the peak of the distribution lies near one-half of the flux limit for the two-image systems, and near one-tenth of the flux limit for the four-image systems. The bulk of the lenses seen in the JVAS sample come from sources that are fainter than the existing redshift surveys ($S < 300$ mJy), and those with brighter sources lie in the region where the redshift surveys are incomplete ($S < 500$ mJy). Almost all the CLASS lenses are from sources fainter than the flux limits of existing redshift surveys. Figure 5 shows the variation of the mean source redshift with flux for several of the models, as well as the constraints from redshift surveys of bright sources. The numbers of lenses found in the various JVAS models are strongly correlated with the mean redshifts of 50–200 mJy sources.

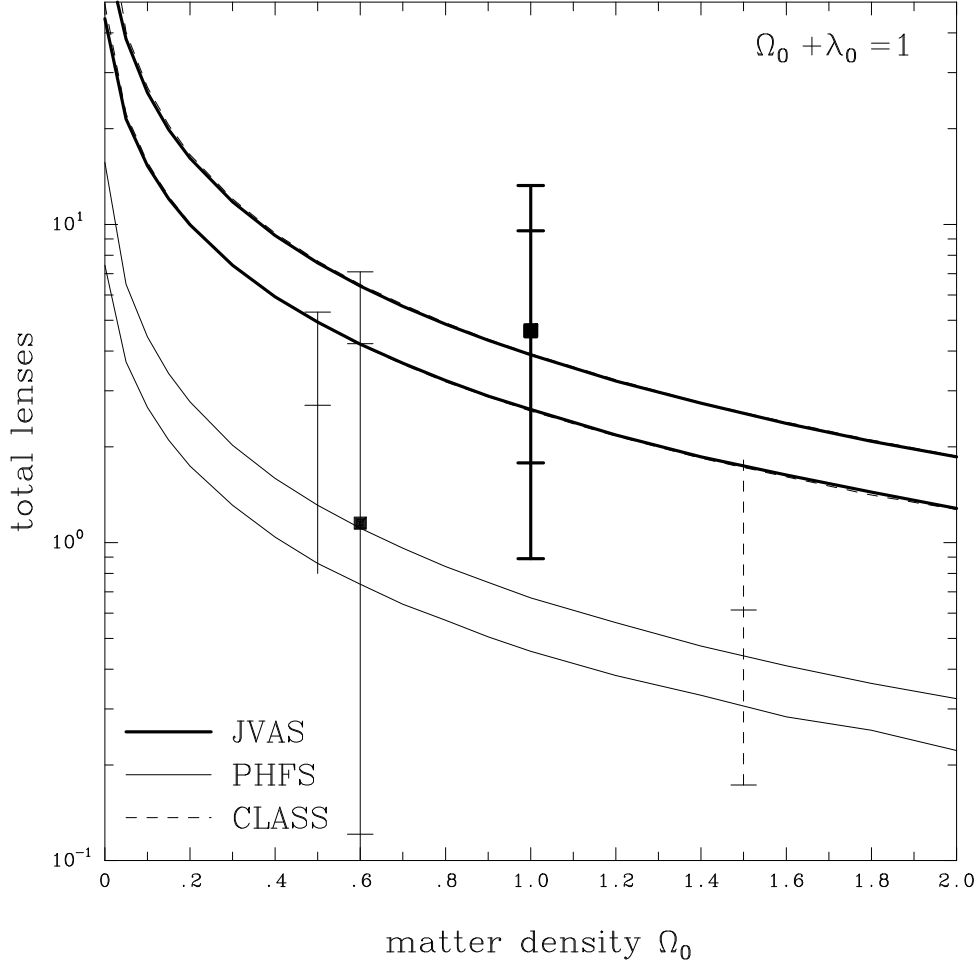


Fig. 2.— The expected numbers of lenses in the JVAS (heavy solid line), CLASS (dashed line, under heavy solid), and PHFS (light solid line) flat spectrum lens surveys as a function of the matter density Ω_0 in flat cosmological models with a cosmological constant ($\Omega_0 + \lambda_0 = 1$). The upper (lower) line of each pair is for Model 05 (Model 01). The JVAS error bar (heavy solid) shows the maximum likelihood value, and the 90% and 99% confidence intervals. The CLASS error bar (dashed) shows where the Poisson probability of finding 2 or more lenses exceeds 1% (lower bar), 10% (upper bar), and 50% (upper tip of line). The two PHFS error bars show either the maximum likelihood limits if the survey contains one lens, or the 1% (upper bar), 10% (lower bar), and 50% (lower tip of line) Poisson limits for finding no lenses. The limits for the surveys are corrected for separations and do not include extended sources. There is no significance to the location of the error bars in Ω_0 .

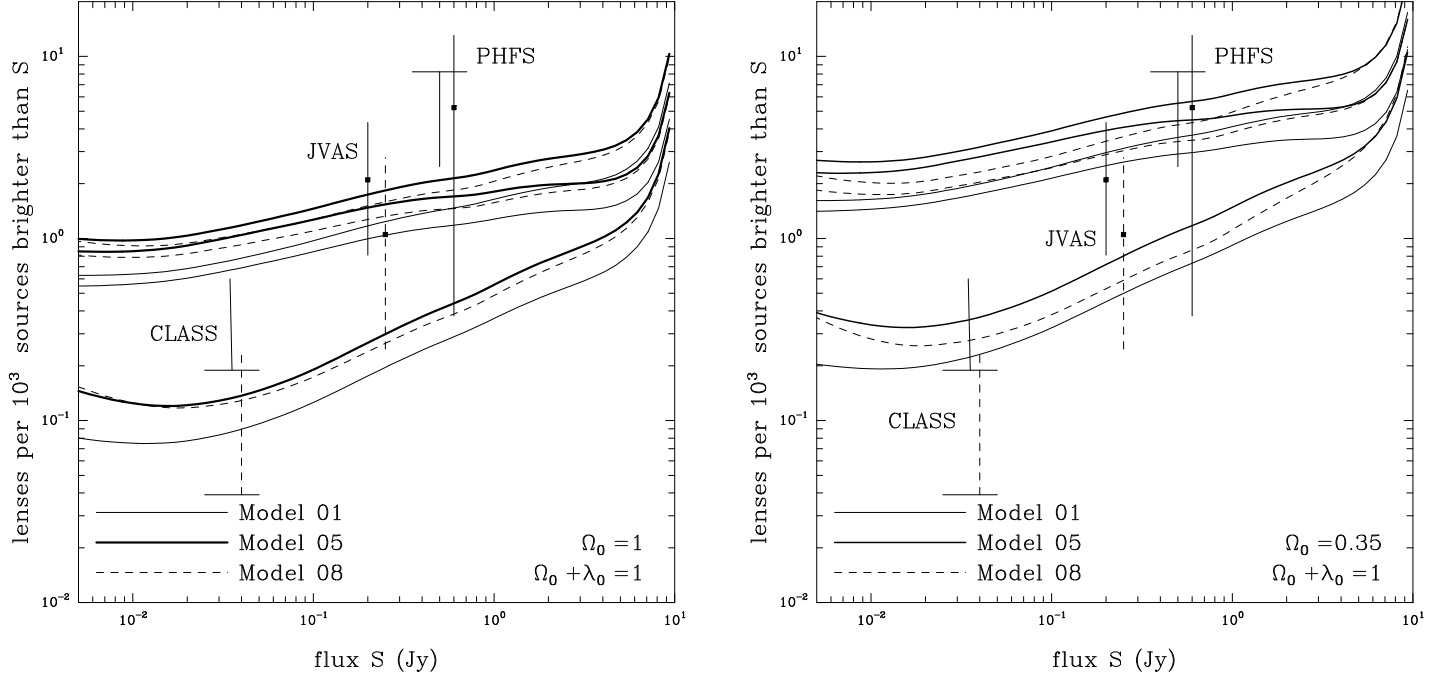


Fig. 3.— The expected number of lenses per 10^3 sources brighter than flux limit S for Models 01 (light solid), 05 (heavy solid), and 08 (dashed) in either an $\Omega_0 = 1$ (left) or an $\Omega_0 = 0.35$ (right) flat cosmological model. Three curves are shown for each model: the top curve is the total number of lenses, the middle curve is the number of two-image lenses, and the lower curve is the number of four-image lenses. For the JVAS survey ($S = 0.2$ Jy) the maximum likelihood (filled point) and 90% confidence limits are shown on the total number of lenses (solid) and the number of four-image lenses (dashed, offset). For the CLASS survey ($S = 25$ to $S = 50$ mJy) the horizontal line marks the limit for a 10% Poisson probability of finding at least two lenses (solid) or at least one four-image lens (dashed, offset). The vertical lines extend to the point where there is a 50% Poisson probability. For the PHFS sample ($S = 0.5$ Jy), the upper limit (left) marks the point where there is a 10% probability of finding no lenses in the sample, and the line extends to the point where there is a 50% probability of finding no lenses. The error bar (right, offset) shows the maximum likelihood value and 90% confidence range if the PHFS sample were to contain one lens.

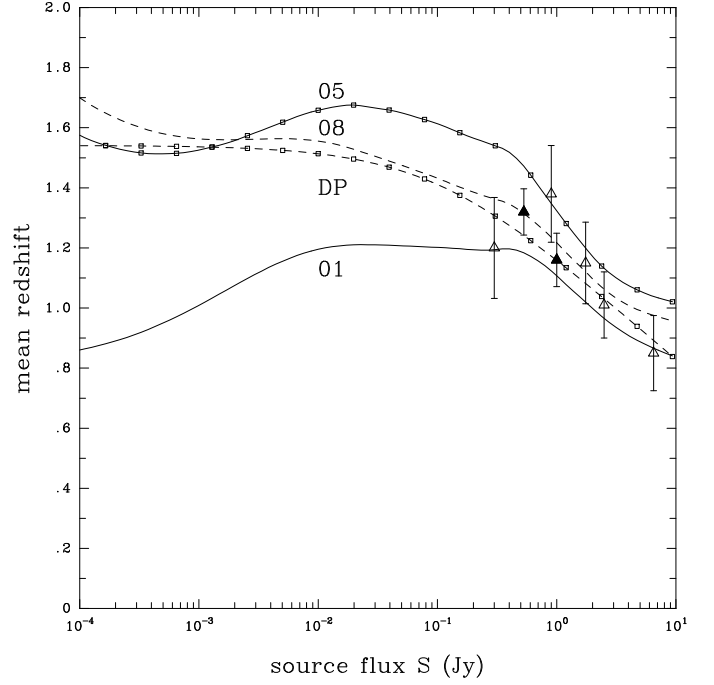
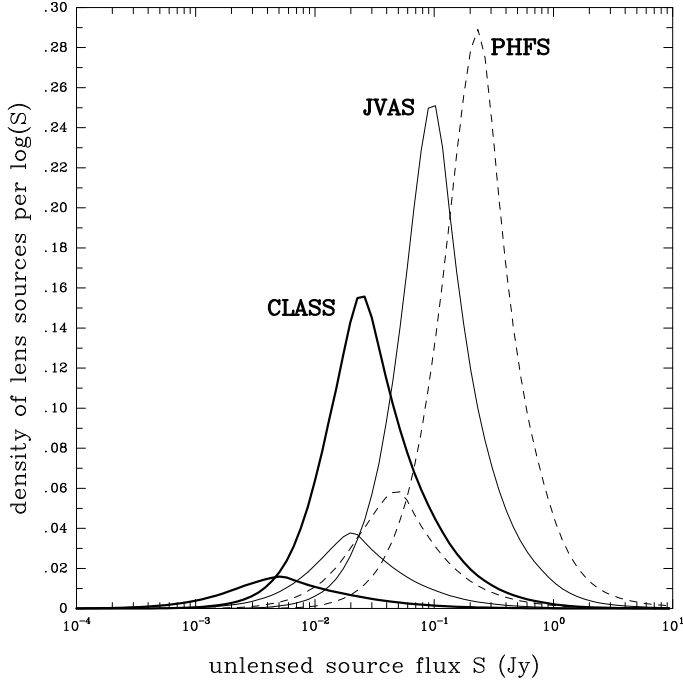


Fig. 4.— (Left) The unlensed flux distribution of lensed sources for the PHFS (dashed), JVAS (solid), and CLASS (heavy solid) samples in Model 01. The higher peak in each pair is for the two-image systems, and the lower peak is for the four-image systems. The vertical scale is the number of lenses per 10^3 sources per $\log S$.

Fig. 5.— (Right) Mean source redshifts as a function of source flux for Model 01 (solid), 05 (solid/points), 08 (dashed), and Dunlop & Peacock (1990) (dashed/points). The error bars show the mean redshift and its uncertainty in the existing redshift surveys, where the open triangles are the distributions from Dunlop & Peacock (1990), and the solid triangles are the CJI and CJII distributions. The curve for Model 05 is the mean for the distribution without the completeness corrections – adding the corrections shifts the curve downwards and brings it into better agreement with the data.

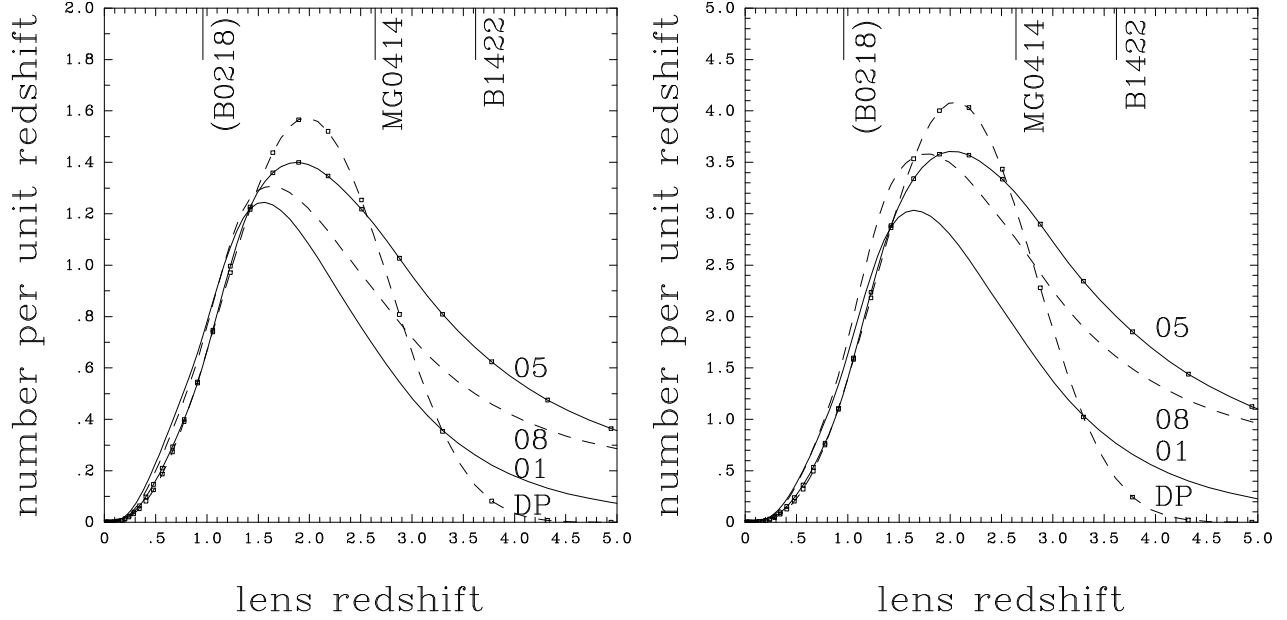


Fig. 6.— Lens (source) redshift distributions in the JVAS survey for $\Omega_0 = 1$ (left) or $\Omega_0 = 0.35$ (right) flat cosmological models. The distributions are shown for Model 01 (solid), 05 (solid/points), 08 (dashed), and Dunlop & Peacock (1990) (dashed/points). The known source redshifts are marked and labeled at the top (the redshift of B0218 is tentative).

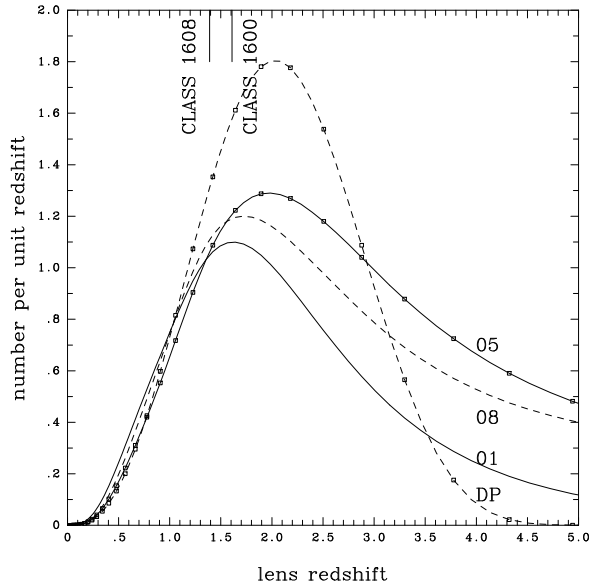


Fig. 7.— Lens (source) redshift distributions in the CLASS survey for $\Omega_0 = 1$. The distributions are shown for Model 01 (solid), 05 (solid/points), 08 (dashed), and Dunlop & Peacock (1990) (dashed/points). The known source redshifts are marked and labeled at the top.

The other way to reduce the uncertainties in the RLF is to use the properties of the observed lenses, although using the lenses adds many complications because their properties combine the effects of the RLF, the cosmological model, and the properties and distribution of the lens galaxies. Nonetheless, the flux and redshift distributions of the lenses may be as useful a constraint on the RLF as direct surveys once there are larger numbers of lenses.

The flux distributions of the lenses in the various models and different cosmologies are very similar and consistent with the observed flux distribution of the lenses. The similarity arises because the lens probability curves (see Figure 3) have almost identical shapes as a function of flux. When normalized to the observed number of lenses, the integral distribution of lens fluxes are indistinguishable. Even over longer flux baselines (e.g. JVAS versus CLASS), the relative numbers of lenses show little change from model to model.

The redshift distributions, however, differ markedly, as Figures 6 and 7 show. Models predicting larger numbers of lenses generally have higher lens redshifts, independent of the cosmological model. Models where the completeness decreases with source redshift (e.g. Model 05) allow many high redshift lenses ($z > 4$). All our models predict some $4 < z < 5$ lenses, in contrast to the sharp cutoff in the Dunlop & Peacock (1990) model. The smoothing function we use does not truncate the number density of high redshift sources as abruptly simply because a more gradual reduction in the number of sources is both smoother and generally compatible with the absence of such sources in the existing redshift surveys. For example, in Model 08 (05), the total number of objects expected in the highest redshift bin ($4 < z < 5.16$) for all seven surveys is 4.6 (3.0) and the surveys found no objects. The next highest redshift bin ($3.5 < z < 4$) has a predicted content of 4.1 (3.3) objects and the surveys found 4 objects. Although the expected numbers of objects are similar, the source density in the higher redshift bin is more than two times lower because of the change in the bin widths. For comparison, the Dunlop & Peacock (1990) model predicts 0.034 sources in the high redshift bin and 0.45 sources in the next lower redshift bin. The Poisson likelihoods of the source counts in these bins for Model 08, Model 05, and Dunlop & Peacock (1990) are 0.2%, 0.9%, and 0.1% respectively, compared to a peak Poisson likelihood of 20%. Our distributions decline too slowly, but the Dunlop & Peacock (1990) distribution declines too rapidly. Moreover, the whole problem may be dominated by redshift dependent incompleteness. The lensing optical depth rises steeply with redshift, so the lensed sample will show a weaker drop off with source redshift than the unlensed sample. While the $z > 4$ sources represent 1% or less of the sources in the redshift surveys, they can be 10-20% of the lensed sources if the cutoff in the RLF at high redshift is less steep than the Dunlop & Peacock (1990) model predicts. The three redshifts in the JVAS sample are compatible with almost any of these distributions, except possibly the Dunlop & Peacock (1990) distribution where the $z = 3.62$ redshift of B 1422+231 is unlikely. Figure

7 shows the expected lensed source redshift distribution for $\Omega_0 = 1$ in the CLASS survey. The distributions are little changed from the JVAS distribution. The continued absence (or discovery) of high redshift lensed sources ($z > 4$), may be a more powerful constraint on the high redshift RLF than direct redshift surveys.

5. Models Constrained to Find Fixed Numbers of Lenses

While we explored a range of smoothing terms in §4, they may not be the terms to find the maximum, physically allowable range for the number of lenses. For example, none of the nine models in Table 1 reached four observable lenses in the JVAS sample. We find little difference if we give the lenses their true statistical weight ($\lambda_L = 1$) because there are so few lenses. We can, however, regard the lensing terms as a type of smoothing by setting $\lambda_L = 10^4$, and then converging the model until $L_{data} = 147$ by adjusting the Lagrangian multiplier of the smoothing λ_U . In this section we explore the properties of RLF models constrained to produce exactly two, four or six observable lenses in the JVAS survey after correcting for resolution and including only compact sources for flat cosmological models with $0 < \Omega_0 < 2$.

Although constrained to have $L_{data} = 147$, the models do not necessarily agree with all the individual constraints. If one data set is poorly fit because it cannot be satisfied given the lensing constraint, the target value of L_{data} can still be reached by overfitting the other data.² For the models constrained to find four lenses, the poorly fit data are always the two lowest flux redshift distributions, the CJII sample and the Parkes Selected Area Sample. For small matter densities, the mean redshift is too low to agree with the data, and for high matter densities it is too high. Figure 8 shows the likelihood ratios for fitting the CJII and PSAS samples as a function of Ω_0 . We can find models with exactly four lenses that are consistent with these redshift distributions for $0.5 \lesssim \Omega_0 \lesssim 1.4$ at 99% confidence if we simply use the likelihood ratio to determine the confidence intervals. In short, finding four lenses in 2200 sources is compatible with a substantial positive (negative) cosmological constant only if the true lensing rate is significantly higher (lower) than in the current sample.

Since the models are constrained to fit the observed number of lenses exactly and are compatible with the flux and redshift constraints except for the most extreme cosmological models, we must find some other means of distinguishing between models. When the

²We can avoid this by using separate Lagrange multipliers for each constraint, and then adjusting these multipliers until each individual constraint has a satisfactory fit.

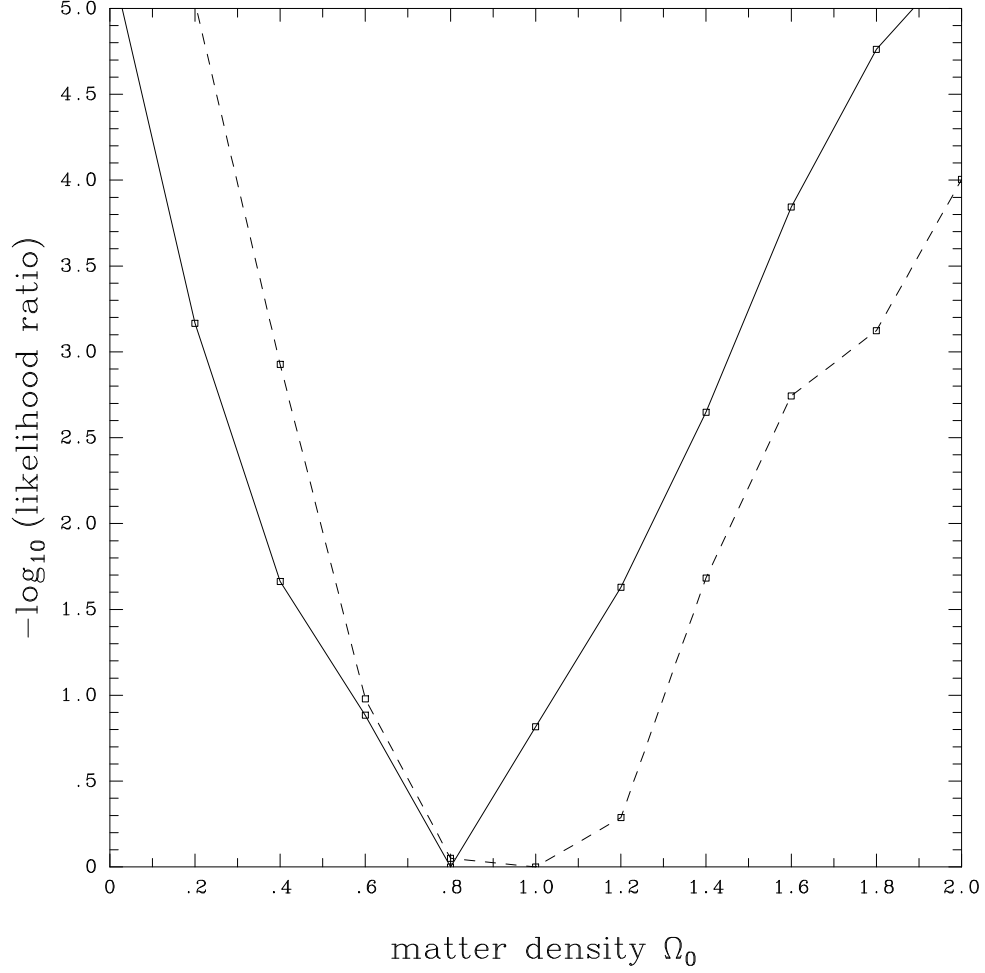


Fig. 8.— The likelihood ratio $\log L/L_{max}$ of fitting the CJII and PSAS redshift distributions as a function of the matter density Ω_0 in flat cosmologies for models constrained to have 4 JVAS lenses. The solid line uses the smoothing parameters of Model 01, and the dashed uses those of Model 05.

number of JVAS lenses is fixed, the numbers of PHFS and CLASS lenses are also nearly fixed (except for $\Omega_0 \lesssim 0.2$). The differences between models are found in the redshift distributions of lensed and unlensed sources.

Both redshift distributions have strong variations with the cosmological model when the number of lenses is fixed. Figure 9 shows the redshift distribution of lensed sources for models constrained to have four lenses (Model 01 smoothing terms) as a function of the matter density. Since the number counts data constrain the total number of sources at any given flux, and the shape of the magnification probability distribution is independent of the cosmological model, the only way to hold the number of lenses fixed is by adjusting the redshift distribution. Models with a large positive cosmological constant have high optical depths, driving down the mean redshift, while models with a large negative cosmological constant have low optical depths, driving up the mean redshift. The same effect can be seen in the mean redshift of unlensed sources shown in Figure 10. We can also search for models in a fixed cosmology producing different numbers of lenses. Figures 9 and 10 also show the properties of $\Omega_0 = 1$ models (with Model 01 smoothing terms) that produce either two or six lenses in the JVAS sample. The two lens model is consistent with all the RLF constraints, but the six lens model fits the PSAS redshift data poorly.

This experiment, using the lensing constraints as a type of smoothing term, demonstrates that the range for the expected number of lenses in the JVAS survey is broader than the range we found for the models in Table 1. There are plausible, consistent RLF models that produce 4 observable lenses in the JVAS sample for $\Omega_0 = 1$. Most of the uncertainty can be eliminated by determining the source redshift distribution for fluxes between 10 and 300 mJy. Completing the surveys in the 300 to 1000 mJy flux range (the CJI, CJII, and PSAS surveys) will help, but most lenses in the JVAS sample come from the fainter flux range.

6. The “Ellipticity Crisis”

King & Browne (1996) point out that the JVAS sample contains an anomalously high number of four-image lenses, and that there are signs of a similar problem in the CLASS sample. The observed fraction (again neglecting B 1938+666, which has both two- and four-image parts) is one in two, while the predicted ratio is one in five for our standard model. The two issues we must consider are whether the problem exists, and how to solve it.

Does a problem exist? For Model 01 in §4, including the separation completeness factor

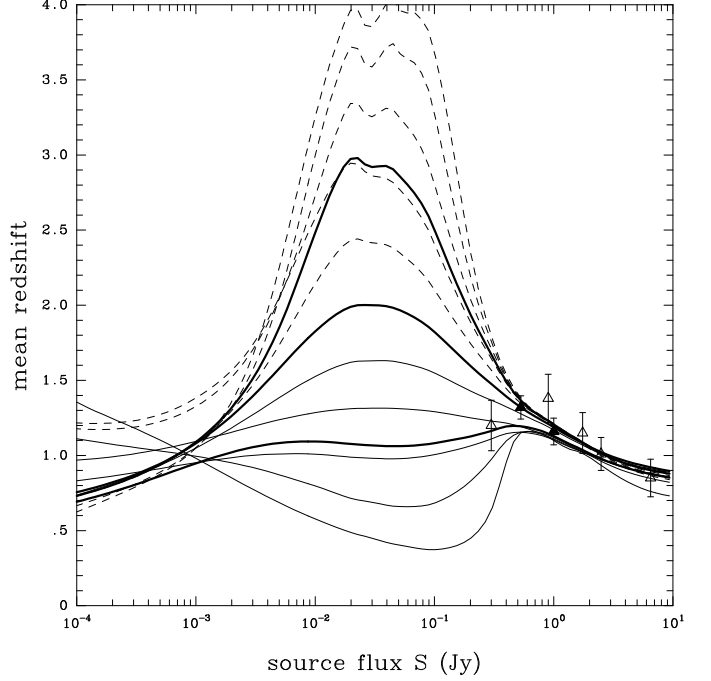
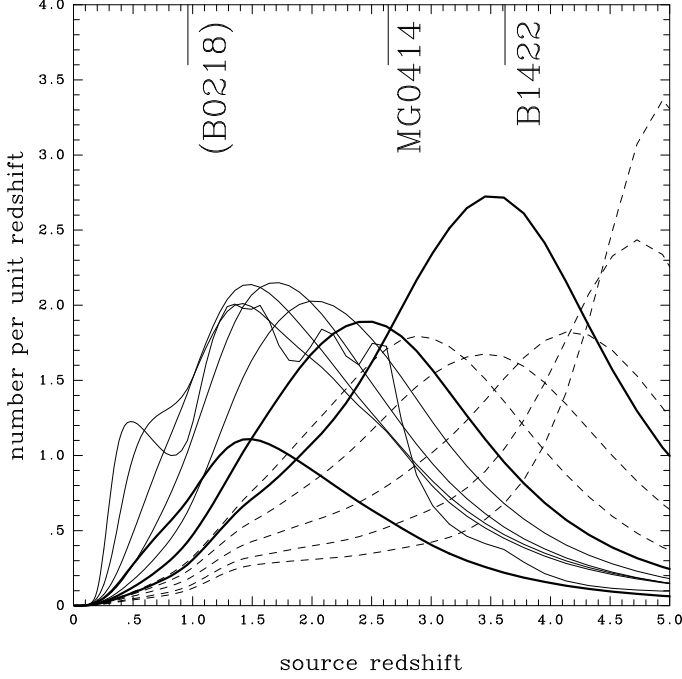


Fig. 9.— (Left) The redshift distribution of lensed sources constrained to have a fixed number of JVAS lenses. The heavy solid lines have $\Omega_0 = 1$ and produce 2, 4, or 6 lenses in order of increasing mean redshift. The light solid lines with peaks shifting to lower redshifts are constrained to produce four lenses and have $\Omega_0 = 0.8, 0.6, 0.4, 0.2$, and 0.0 , while the dashed lines with peaks shifting to higher redshifts are constrained to produce four lenses and have $\Omega_0 = 1.2, 1.4, 1.6, 1.8$, and 2.0 , all with $\Omega_0 + \lambda_0 = 1$. The wiggles in the low Ω_0 models are caused by the overfitting needed to reach $L_{data} = 147$. We used the Model 01 smoothing terms.

Fig. 10.— (Right) The mean redshift of unlensed sources as a function of source flux for RLF models constrained to produce a fixed number of JVAS lenses using the Model 01 smoothing terms. The mean redshifts from the seven redshift constraints are shown by the points. The heavy solid lines have $\Omega_0 = 1$ and 2, 4, or 6 lenses in order of increasing mean redshift, the solid lines with peaks shifting to lower redshifts have 4 lenses and $\Omega_0 = 0.8, 0.6, 0.4, 0.2$, and 0.0 , while the dashed lines with peaks shifting to higher redshifts have 4 lenses and $\Omega_0 = 1.2, 1.4, 1.6, 1.8$, and 2.0 , all with $\Omega_0 + \lambda_0 = 1$.

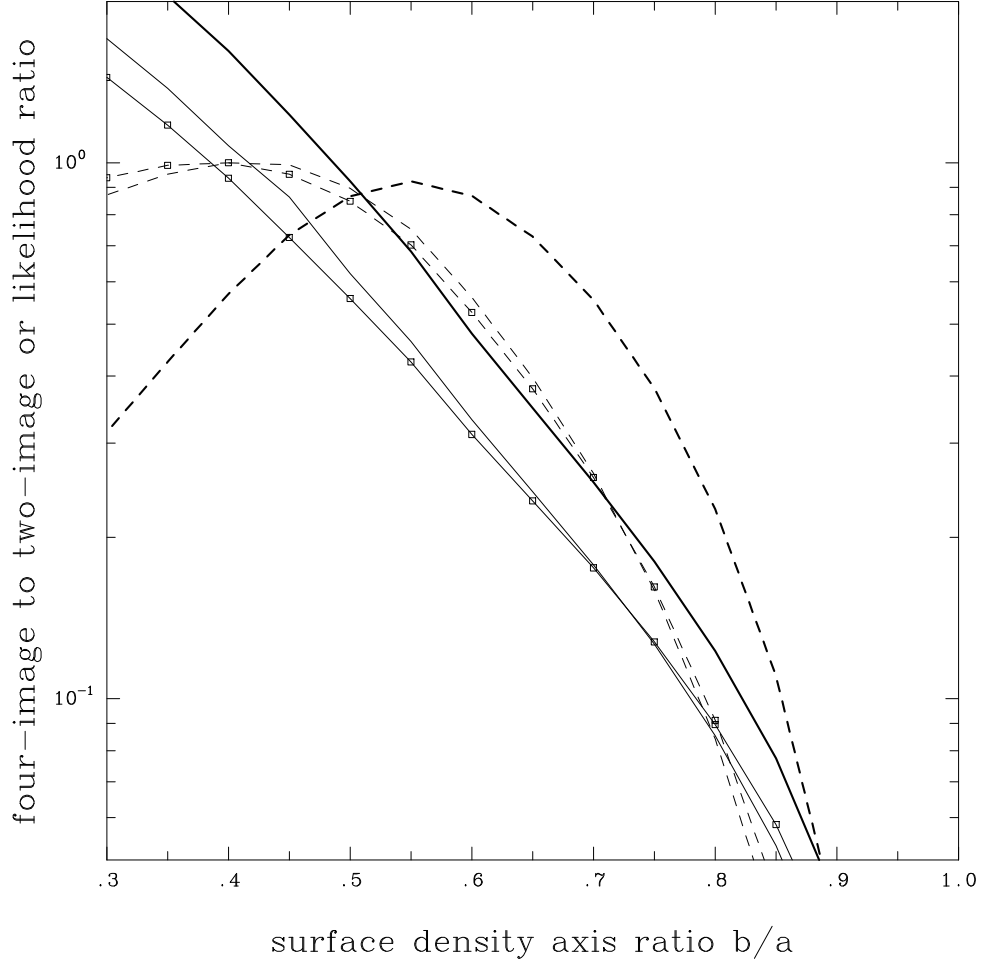


Fig. 11.— The four-image to two-image number ratio as a function of galaxy axis ratio b/a (solid curves) and the corresponding maximum likelihood ratios (dashed curves). The light solid curves show the ratio for Model 01 (no points) and a model with 4 lenses and the Model 01 smoothing curves (with points), and the heavy solid line shows the equivalent ratio for the quasar surveys discussed by Kochanek (1996). The quasar surveys contain 3 two-image and 2 four-image lenses, while the JVAS survey contains 2 two-image and 2 four-image lenses of compact sources. The corresponding dashed lines show the likelihood ratio for the models to produce the observed numbers of two- and four-image systems when constrained to have the observed total number of lenses.

and dropping the extended sources, we expect 1.92 two-image and 0.34 four-image lenses in the observed sample. The Poisson probability of finding at least as many four-image as two-image lenses given these expectation values is 24% if we do not constrain the distributions to have four lenses, and 11% for samples containing four lenses. For Model 05, we expect 2.83 two-image and 0.52 four-image lenses, and the probability of finding at least as many four-image as two-image systems is 15% if unconstrained, and 12% if constrained to have four images (see Figure 3). In the $\Omega_0 = 1$ model constrained to have four lenses (see §5) we expect 3.36 two-image and 0.62 four-image systems, with a 12% chance of having at least as many four-image as two-image systems.

So far, all models were computed using the statistical predictions from a uniform distribution of galaxies with axis ratios between $b/a = 0$ and $b/a = 0.5$. This “standard” model has a two-image to four-image number ratio comparable to the ratio for a model with an axis ratio between $b/a = 0.65$ and 0.70 (see Figure 1). Figure 11 shows the expected ratio of four-image to two-image lenses in the JVAS survey as a function of the axis ratio of the surface density, as well as the equivalent results for the quasar lens sample used by Kochanek (1996), which contains three two-image and two four-image lenses. The quasars have more four-image lenses for a given ellipticity because the magnification bias of the sample is greater (see Kochanek 1991, Wallington & Narayan 1993, Kassiola & Kovner 1993). To match the observed JVAS ratio of 1:1 requires $b/a = 0.4$, much more flattened than a typical elliptical galaxy (see Ryden 1992). We quantify the agreement using the maximum likelihood ratio to estimate confidence limits from the Poisson probability of finding 2 two-image and 2 four-image lenses in a sample containing four lenses in total. The largest axis ratios agreeing with the data at the $1\text{-}\sigma$, 90% confidence, and $2\text{-}\sigma$ confidence limits have $b/a \simeq 0.55$, $b/a \simeq 0.70$, and $b/a \simeq 0.75$ respectively. Our standard model for the ellipticity distribution lies near the 90% confidence limit.

The quasar model matches the observed ratio at an axis ratio of $b/a = 0.55$, which is not as elliptical as the best fit to the JVAS data, but more elliptical than our standard model. The $1\text{-}\sigma$ and 90% maximum likelihood confidence limits for this model are $0.35 \lesssim b/a \lesssim 0.70$ and $0.25 \lesssim b/a \lesssim 0.75$. The standard model is still too circular, but only at the $1\text{-}\sigma$ level. The radio and quasar ellipticity probability distributions are perfectly compatible, and if we examine the joint probability distribution we find that the best fit is $b/a = 0.50$, with a $1\text{-}\sigma$ range of $0.35 \lesssim b/a \lesssim 0.60$ and a 90% confidence range of $0.25 \lesssim b/a \lesssim 0.75$. The standard model lies between the $1\text{-}\sigma$ and 90% confidence limits.

In short, the observed ratio of two-image to four-image lenses is somewhat, but not significantly, unlikely. There are, however, other signs of ellipticity problems from highly elliptical lens models or gross disagreements between the models and the observed lens

galaxy (see Kochanek (1991), or Ratnatunga et al. 1995 for some examples), a point strongly emphasized by Schechter (1996). Some solutions to the statistical ellipticity problem help the model ellipticity problem, but not all.

The statistical discrepancy can be alleviated by adding a core radius to the lens models, which will mostly affect the numbers of two-image systems, or by unmodeled systematic biases in the surveys against recognizing two-image systems. These two effects reduce the number of two-image lenses while leaving the number of four-image lenses unchanged for a fixed RLF model. However, the systematic uncertainties associated with the RLF can easily compensate for the variations in the expected number of lenses to keep the models in agreement with plausible cosmological models (as demonstrated in §5). These are viable solutions to the statistical ellipticity problem, but they cannot explain high ellipticities in individual lens models.

We can also use the RLF to increase the number of four-image systems. Figure 4 shows that the two- and four-image systems in a particular survey are produced by sources with different fluxes. By boosting the number of faint sources in the four-image peak relative to the number of sources in the two-image peak, we increase the relative number of four-image systems. This effect causes the higher ratio of four- to two-image systems predicted in the quasar surveys (see Figure 11), because the bright quasar ($m \lesssim 18$ B mags) LF is steeper than the RLF. Note, however, that the four-image source peak for the JVAS survey lies in the middle of the two-image source peak for the CLASS survey. Models boosting the ratio in the JVAS survey usually reduce the ratio in the CLASS survey. If we change the likelihood for the lensing model to separately fit the numbers of two- and four-image systems, we can significantly increase the ratio.

We have not included spiral galaxies in our calculations, but they cannot solve the ellipticity problem even if they are very flattened. Current evidence (see Sackett 1996) suggests that spiral halos are nearly axisymmetric and oblate, with a three-dimensional axis ratio of ~ 0.5 . The projected two-dimensional axis ratios will be higher. Spiral galaxies produce only a fraction $x = 0.15$ to 0.20 of the optical depth produced by the early type galaxies – their lower average mass outweighs their higher number density (see Fukugita & Turner 1990, Maoz & Rix 1993, Kochanek 1993, 1996). If fractions r_e and r_s of E/S0 and spiral lenses are four-image lenses respectively, then the overall fraction of four-image lenses is $r = (r_e + xr_s)/(1 + x) \simeq 0.83r_e + 0.17r_s$ (for $x = 0.2$). If we use the canonical $r_e = 0.16$ from our typical RLF models, then $r_s = 0.5 + 0.35/x = 2.25$ for $x = 0.2$ is needed for the spirals to explain equal numbers of two- and four-image lenses. Such a value for r_s implies a surface density axis ratio smaller than $b/a = 0.3$, contradicting the dynamical estimates of the properties of spiral halos. Thus, spiral galaxies are of little help in explaining the

ellipticity problem.

7. Conclusions

The results of the JVAS lens survey (see Patnaik 1994, King & Browne 1996) are consistent with models for the statistics of lensed quasars (Kochanek 1996), although the cosmological uncertainties are broader because of the systematic uncertainties in the RLF (radio luminosity function). This agreement is a remarkable affirmation of lens statistical models, since the only common assumption is the model for the number and mass distribution of lens galaxies. There are four JVAS lenses produced by compact sources, and in an $\Omega_0 = 1$ cosmological we predicted between 2.3 and 3.4 lenses for a series of RLF models consistent with observational constraints. In fact, there is no problem finding a model RLF that produces exactly four observable lenses in this sample for $\Omega_0 = 1$. In flat cosmological models ($\Omega_0 + \lambda_0 = 1$) the systematic uncertainties are consistent with a broad range of values for the matter density, with $0.20 \lesssim \Omega_0 \lesssim 2.0$ at 90% confidence.

In addition to the JVAS survey, we estimated the number of lenses expected in the CLASS and PHFS surveys. So far, the CLASS survey (Myers 1996, Myers et al. 1995, Jackson et al. 1995) has found two lenses in a larger, fainter sample than the JVAS survey. Our models predict that the number of lenses expected in the first part of the CLASS survey is approximately equal to the number expected in the JVAS survey. Although the CLASS survey contains more sources, the lensing probability is a declining function of source flux. The PHFS survey (Webster et al. 1996) is examining a much smaller sample of brighter sources, and our models predict only 0.3 to 0.6 lenses for $\Omega_0 = 1$. There are too few lensed source redshifts to distinguish between RLF models in the current samples, but they are a promising means of constraining models. The flux distribution of the lensed sources is consistent with the model predictions.

The systematic uncertainties in the expected number of lenses and the RLF model are created by the absence of redshift information for (unlensed) sources fainter than 300 mJy. The source of a typical JVAS lens is a 50–200 mJy source, and the source of a typical CLASS lens is a 10–50 mJy source, well below the fluxes with even partial redshift distributions. The redshift distribution of the sources at these fluxes is largely constructed from assumptions about smoothness and evolution, and the resulting uncertainty in the mean redshift of the sources permits large variations in the expected number of lenses. If, for example, we examine model RLFs that produce exactly 4 JVAS lenses, the mean redshift of a 50 mJy source varies from 0.4 for $\Omega_0 = 0$, to 1.9 for $\Omega_0 = 1$, to almost 4.0 for $\Omega_0 = 2$ in flat cosmologies with a cosmological constant ($\Omega_0 + \lambda_0 = 1$). The extremes for

the mean redshift are implausible, but they serve to illustrate the direct relation between mean source redshift and cosmological uncertainties. *Using the flat spectrum radio lens surveys to study the cosmological model depends on determining the redshift distribution of radio sources in the flux range from 10 to 300 mJy.* While it is helpful to complete the existing brighter redshift surveys (CJI and CJII (e.g. Taylor et al. (1994), Henstock et al. (1995), Thakkar et al. (1995)), PHFS (Parkes Half-Jansky Flat-Spectrum Survey, Webster et al. 1996), and PSAS (Parkes Selected Areas Survey, Dunlop et al. 1986, Dunlop et al. 1986, Allington-Smith et al. 1991) samples), they are at the wrong fluxes to eliminate the cosmological uncertainties. Because the redshift variations are so large, relatively small (50 sources) redshift surveys of modest completeness (80% or better) can eliminate most of the uncertainties.

As noted by King & Bowne (1996), the number of four-image lenses in the JVAS survey (2 of 4 compact-source lenses) is significantly greater than the 14-16% predicted by theoretical models using ellipticities typical of E and S0 galaxies. A uniform distribution of lenses in axis ratio from $b/a = 0.5$ to $b/a = 1.0$ (roughly the distribution for E and S0 galaxies, e.g. Schechter (1987), Ryden (1992)) produces the same numbers of four-image lenses as a galaxy with an axis ratio of $b/a \simeq 0.65$. A model that produces the observed ratio of four-image to two-image lenses is too elliptical, with an axis ratio of $b/a \simeq 0.4$. The discrepancy is significant only at the 90% confidence level, since the 1- σ , 90% confidence, and 2- σ upper limits on the axis ratio are $b/a = 0.55$, 0.70, and 0.75 respectively. Fitting the number of four-image lenses found in quasar lens surveys (see Kochanek 1991, 1996, Wallington & Narayan 1993, Kassiola & Kovner 1993) also requires higher than expected ellipticities, but the discrepancy is significant only at the 1- σ confidence level. The ellipticity estimates for the radio and quasar lenses are perfectly compatible, and the joint distribution has a best fit axis ratio of $b/a = 0.5$ and a 90% confidence range of $0.25 \lesssim b/a \lesssim 0.65$. While the best fitting lens models are more elliptical than expected for E/S0 galaxies, the Poisson uncertainties are so broad that the significance of the discrepancy is only at the 90% confidence level.

There are four plausible solutions to the ellipticity problem. The first solution is that the problem does not exist, since the statistical significance of the disagreement is low. The second solution is that systematic errors in the calculations lead to the discrepancy. For example, there are many reasons our selection effects model may overestimate the detectability of two-image lenses. The RLF allows enough freedom in the total number of lenses to halve the number of detectable two-image lenses and still remain consistent with the lensing and RLF constraints. Schechter (1996) emphasizes that there is also a problem with models of individual lenses being too elliptical, and neither of these solutions to the statistical ellipticity problem can address this. The third solution is that the dark matter

halos of early type galaxies are more elliptical than the light, and the fourth solution is that external shear perturbations from structure near the lens or along the line of sight augment the intrinsic ellipticities of the lens galaxies (e.g. Kochanek & Apostolakis 1988, Bar-Kana 1996).

Acknowledgements: The author thanks P. Schechter for discussions and E. Falco for comments. The research was supported by the Alfred P. Sloan Foundation and NSF grant AST 94-01722.

REFERENCES

- Allington-Smith, J.R., Peacock, J.A., & Dunlop, J.S., 1991, MNRAS, 253, 287
- Altschuler, D.R., 1986, A&ASuppl, 65, 267
- Bar-Kana, R., 1996, *astro-ph/9511056 preprint*
- Bennett, C.L., Lawrence, C.R., & Burke, B.F., 1985, ApJ, 299, 373
- Blandford, R.D., & Narayan, R. 1986, ApJ, 310, 568
- Breimer, T.G., & Sanders, R.H., 1993, A&A, 274, 96
- Burke, B.F., Lehàr, J., & Conner, S.R., 1992, in Gravitational Lenses, ed. R. Kayser, T. Schramm, & L. Nieser (Springer: Berlin) 237
- Carroll, S.M., Press, W.H., & Turner, E.L., 1992, ARA&A, 30, 499
- Condon, J.J., 1989, ApJ, 338, 13
- Condon, J.J., & Ledden, J.E., 1981, AJ, 86, 643
- Donnelly, R.H., Partridge, R.B., & Windhorst, R.A., 1987, ApJ, 321, 94
- Dunlop, J.S., 1994, in Frontiers of Space and Ground-Based Astronomy, eds., W. Wamsteker et al. (Kluwer: Dordrecht) 395
- Dunlop, J.S., Peacock, J.A., Savage, A., & Carrie, D.R., 1986, MNRAS, 218, 31
- Dunlop, J.S., Peacock, J.A., Savage, A., Lilly, S.J., Heasley, J.N., & Simon, A.J.B., 1989, MNRAS, 238, 1171
- Dunlop, J.S., & Peacock, J.A., 1990, MNRAS, 247, 19
- Driver, S.P., Windhorst, R.A., Phillipps, S., & Bristow, D., 1995, *astro-ph/9511141 preprint*
- Faber, S.M., & Jackson, R.E., 1976, ApJ, 204, 668
- Fomalont, E.B., Kellerman, K.I., Wall, J.V., & Weistrop, D., 1984, Science, 225, 23

- Fomalont, E.B., Windhorst, R.A., Kristian, J.A., & Kellerman, K.I., 1991, *AJ*, 102, 1258
- Franx, M., 1993, in *Galactic Bulges*, ed. H. Dejonghe & H.J. Habing (Dordrecht: Kluwer) 243
- Fukugita, M., Futamase, T., & Kasai, M., 1990, *MNRAS*, 246, 24p
- Fukugita, M., & Turner, E.L., 1991, *MNRAS*, 253, 99
- Gregory, P.C., & Condon, J.J., 1991, *ApJS*, 75, 1011
- Henstock, D.R., Browne, I.W.A., Wilkinson, P.N., Taylor, G.B., Vermeulen, R.C., Pearson, T.J., & Readhead, R.C.S., 1995, *ApJS*, 100, 1
- Henstock, D.R., Browne, I.W.A., & Wilkinson, P.N., 1994, *Spectrum*, 4, ??
- Hewitt, J.N., Turner, E.L., Schneider, D.P., Burke, B.F., Langston, G.I., & Lawrence, C.R., 1988, *Nature*, 333, 537
- Hogg, D.W., & Blandford, R.D., 1994, *MNRAS*, 268, 889
- Jackson, N., de Bruyn, A.G., Myers, S., Bremer, M.N., Miley, G.K., Schilizzi, R.T., Browne, I.W.A., Nair, S., Wilkinson, P.N., Blandford, R.D., Pearson, T.J., & Readhead, A.C.S., 1995, *MNRAS*, 274, L25
- Kassiola, A., & Kovner, I., 1993, *ApJ*, 417, 450
- Kellerman, K.I., & Wall, J.V., 1987, in *Observational Cosmology*, eds., A. Hewitt, et al., (Kluwer: Dordrecht) 543
- King, L.J. & Browne, I.W.A., 1996, *MNRAS*, 282, 67
- King, L.J., Browne, I.W.A., Wilkinson, P.N., & Patnaik, A.R., 1996, in *Astrophysical Applications of Gravitational Lensing*, eds., C.S. Kochanek & J.N. Hewitt (Kluwer: Dordrecht) 191
- Kochanek, C.S., 1991, *ApJ*, 379, 517
- Kochanek, C.S., & Lawrence, C.R., 1990, *AJ*, 99, 1700
- Kochanek, C.S., 1993, *ApJ*, 419, 12
- Kochanek, C.S., 1994, *ApJ*, 436, 56
- Kochanek, C.S., 1996, *ApJ*, *in press*.
- Lawrence, C.R., Elston, R., Jannuzi, B.T., & Turner, E.L., 1994, *Caltech preprint*
- Lehár, J., 1991, MIT PhD Thesis
- Lilly, S.J., Tresse, L., Hammer, F., Crampton, D., & Le Fèvre, O., 1995, *ApJ*, 455, 108
- Loveday, J., Peterson, B.A., Efstathiou, G., & Maddox, S.J., 1992, *ApJ*, 390, 338
- Mao, S., 1991, *ApJ*, 380, 9

- Mao, S., & Kochanek, C.S., 1994, *MNRAS*, 268, 569
- Maoz, D., & Rix, H.-W., 1993, *ApJ*, 416, 425
- Marzke, R.O., Geller, M.J., Huchra, J.P., & Corwin, H.G., 1994, *AJ*, 108, 437
- Maslowski, J., Pauliny-Toth, I.I.K., Witzel, A., & Kühr, H., 1981, *A&A*, 95, 285
- Myers, S.T., Fassnacht, C.D., Djorgovski, S.G., et al., 1995, *ApJ*, 447, L5
- Myers, S.T., 1996, in *Astrophysical Applications of Gravitational Lensing*, eds., C.S. Kochanek & J.N. Hewitt (Kluwer: Dordrecht) 317
- Owen, F.N., Condon, J.J., & Ledden, J.E., 1983, *AJ*, 88, 1
- Patnaik, A.R., 1994, in *Gravitational Lenses in the Universe*, ed., J. Surdej, D. Fraipont-Caro, E. Gosset, S. Refsdal, & M. Remy (Liège, Université de Liège) 311
- Patnaik, A.R., Browne, I.W.A., King, L.J., Muxlow, T.W.B., Walsh, D., & Wilkinson, P.N., 1992a, in *Gravitational Lenses*, ed. R. Kayser, T. Schramm, & L. Nieser (Springer: Berlin) 140
- Patnaik, A.R., Browne, I.W.A., Wilkinson, P.N., & Wrobel, J.A., 1992, *MNRAS*, 254, 655
- Pauliny-Toth, I.I.K., Witzel, A., Preuss, E., Kühr, H., Kellerman, K.I., & Fomalont, E.B., 1978, *AJ*, 83, 451
- Peacock, J.A., 1983, *MNRAS*, 202, 615
- Peacock, J.A., 1985, *MNRAS*, 217, 601
- Peacock, J.A., & Wall, J.V., 1981, *MNRAS*, 194, 331
- Polatidis, A.G., Wilkinson, P.N., Xu, W., Readhead, A.C.S., Pearson, T.J., Taylor, G.B., & Vermeulen, R.C., 1994, *ApJS*, 98, 1
- Press, W.H., Teukolsky, S.A., Vetterling, W.T., & Flannery, B.R., 1992, *Numerical Recipes* (Cambridge Univ. Press: Cambridge)
- Ratnatunga, K.U., Ostrander, E.J., Griffiths, R.E., & Im, M., 1995, *ApJ*, 453, L5
- Rix, H.-W., Maoz, D., Turner, E.L., & Fukugita, M., 1994, *ApJ*, 435, 49
- Ryden, B.S., 1992, *ApJ*, 396, 445
- Sackett, P.D., 1996, in *Astrophysical Applications of Gravitational Lensing*, eds., C.S. Kochanek & J.N. Hewitt (Kluwer: Dordrecht) 165
- Schechter, P., 1976, *ApJ*, 203, 297
- Schechter, P., 1987, in *Structure and Dynamics of Elliptical Galaxies*, ed. T. de Zeeuw (Kluwer: Dordrecht) 217
- Schechter, P., 1996, private communication

- Taylor, G.B., Vermeulen, R.C., Pearson, T.J., Readhead, A.C.S., Henstock, D.R., Browne, I.W.A., & Wilkinson, P.N., 1994, *ApJS*, 93, 345
- Thakkar, D.D., Xu, W., Readhead, A.C.S., Pearson, T.J., Henstock, D.R., Browne, I.W.A., & Wilkinson, P.N., 1994, *ApJS*, 98, 33
- Toffolatti, L., Franceschini, A., De Zotti, G., & Danese, L., 1987, *A&A*, 184, 7
- Tomita, K., 1995, *YITP/U94-2 preprint*
- Turner, E.L., 1990, *ApJ*, 365, L43
- Wall, J.V., & Peacock, J.A., 1985, *MNRAS*, 216, 173
- Wallington, S., & Narayan, R., 1993, *ApJ*, 403, 517
- Webster, R.L., Francis, P.J., Holman, B.A., Masci, F.J., Drinkwater, M.J., & Peterson, B.A., 1996, in *Astrophysical Applications of Gravitational Lensing*, eds., C.S. Kochanek & J.N. Hewitt (Kluwer: Dordrecht) 393
- Windhorst, D., Mathis, D., & Neuschaefer, L., 1990, in *Evolution of the Universe of Galaxies*, ed. R.G. Kron (Astron. Soc. of the Pacific: San Francisco) 389
- Witzel, A., Schmidt, J., Pauliny-Toth, I.I.K., & Nauber, U., 1979, *AJ*, 84, 942
- Wrobel, J.M., & Krause, S.W., 1990, *ApJ*, 363, 11
- Xu, W., Readhead, A.C.S., Pearson, T.J., Polatidis, A.G., & Wilkinson, P.N., 1995, *ApJS*, 99, 297